UNIVERSIDADE BEIRA INTERIOR

Delivery of anti-HPV drugs to cervical cancer cells

Versão final após defesa

Miguel Rodrigues Ferreira

Dissertação para obtenção do Grau de Mestre em
Ciências Biomédicas
2º ciclo de estudos

Orientador: Prof.ª Doutora Ângela Maria Almeida de Sousa
Co-orientador: Prof.ª Doutora Diana Rita Barata Costa

novembro de 2022

Declaração de Integridade

Eu, Miguel Rodrigues Ferreira, que abaixo assino, estudante com o número de inscrição M10654 de/o Ciências Biomédicas da Faculdade Ciências da Saúde, declaro ter desenvolvido o presente trabalho e elaborado o presente texto em total consonância com o **Código de Integridades da Universidade da Beira Interior**.

Mais concretamente afirmo não ter incorrido em qualquer das variedades de Fraude Académica, e que aqui declaro conhecer, que em particular atendi à exigida referenciação de frases, extratos, imagens e outras formas de trabalho intelectual, e assumindo assim na íntegra as responsabilidades da autoria.

Universidade da Beira Interior, Covilhã 30 /11 /2022

Assinado por: **Miguel Rodrigues Ferreira**
Num. de Identificação: 15206306
Data: 2022.11.30 01:37:52+00'00'

(assinatura conforme Cartão de Cidadão ou preferencialmente
assinatura digital no documento original se naquele mesmo formato)

Acknowledgments

The elaboration of this master research project concludes this stage of my academic journey. This thesis was only possible thanks to the support of many people who I particularly thank.

First of all, I would like to thank professor doctor Ângela Sousa and professor doctor Diana Costa for the opportunity you gave me to join your working group and for all the support, guidance, motivation and scientific information transmission you gave me during this period. Your criticisms and work suggestions were fundamental to growth as student and future professional. I also thank doctor professor Luis Passarinha for all the support provided in HPLC experiments.

I thank the University of Beira Interior, specially the Health Sciences Research Centre, for the facilities, equipment's and available material. Thanks to all researchers of this centre that contributed for a better work environment and that help me and shared with me important knowledge.

I also thank all my lab colleagues who were always there to support me and share with me their knowledge and friendship. My special thanks to Diana Gomes for helping me along this process, teaching me the techniques applied in this work as well as debating and assisting in all the experiments.

To all my friends who have walked with me all along this path, from all those I met in Porto and who still help and support me, to those I have met over the last few years and have demonstrated that no path can be taken alone, my sincere thanks for all their friendship!

Last but not least, thank to my family for the transmitted force during the year, for always believe in me. To my parents, Isabel Rodrigues and Carlos Ferreira, and brother, Henrique Ferreira, thank you for all the efforts, education, dedication, love and support.

Resumo alargado

O cancro é uma das principais causas de morte a nível mundial, originando mais de 19,3 milhões de casos em 2020, resultando em aproximadamente 10 milhões de mortes. Vários fatores de risco já foram atribuídos ao aparecimento do cancro, sendo a idade, a predisposição genética, a etnia, a exposição ambiental, os estilos de vida e infeções causadas por bactérias, parasitas ou vírus os mais preponderantes.

O vírus do papiloma humano (HPV) é o principal agente causador do desenvolvimento do cancro do colo do útero, o quarto cancro mais comum nas mulheres em todo o mundo e responsável por mais de 340.000 mortes em 2020. A excessiva expressão das oncoproteínas HPV E6 e E7 estão presentes neste tipo de cancro, alterando a regulação do ciclo celular e a sua proliferação mediante o comprometimento das proteínas supressoras de tumor p53 e pRb, respetivamente.

Apesar de já se encontrarem disponíveis vacinas preventivas anti-HPV, a sua administração não é amplamente realizada a toda a população. Desta forma, estão ainda em processo de desenvolvimento terapias para este tipo de cancro, a fim de se conseguir uma cura eficaz. Neste sentido, os flavonoides demonstraram um elevado potencial terapêutico, oferecendo um método eficaz e de baixo custo que permite a sua utilização em países menos desenvolvidos e onde os cuidados de saúde são mais limitados.

A quercetina é o principal flavonoide em usos terapêuticos apresentando inúmeras propriedades anticancerígenas e mostrando particular relevância na terapia do cancro do colo do útero devido ao facto de potenciar a inibição da ação da oncoproteína E6, aumentando assim a expressão da p53 e induzindo assim a apoptose. Contudo, o uso da quercetina é limitado devido à sua insolubilidade em meio aquoso e à sua baixa estabilidade. Assim, a baixa biodisponibilidade da quercetina limita as suas aplicações em terapias do cancro.

Desta forma, esta dissertação de mestrado visa desenvolver sistemas de entrega para a encapsulação da quercetina no sentido de melhorar a sua biodisponibilidade e efeito em células HPV positivas.

Foram formulados e caracterizados três tipos de sistemas, um constituído de éter sulfobutílico β-Ciclodextrina (SBE-β-CD) e os outros dois baseados em quitosano, um

conjugado com tripolifosfato de sódio (TPP) e outro com SBE-β-CD. Os sistemas de entrega de SBE-β-CD/Quercetina apresentaram um tamanho de 2468,33 nm, um índice de polidispersidade (PdI) de 0,123, um potencial zeta de -21,03 mV e uma eficiência de encapsulamento de aproximadamente 100%. Os sistemas de entrega Quitosano/TPP/Quercetina mostraram um tamanho de 325,1 nm, um PdI de 0,371, um potencial zeta de +16,6 mV e uma eficiência de encapsulamento de 10,80%. Finalmente, os sistemas de entrega de Quitosano/SBE-β-CD/Quercetina apresentaram uma dimensão de 272,07 nm, um PdI de 0,287, um potencial zeta de +38,0 mV e uma taxa de encapsulamento de aproximadamente 100%.

Foi realizada microscopia eletrónica de varrimento (SEM) para todos os sistemas de entrega, sendo possível verificar que os sistemas de Quitosano/TPP/Quercetina e Quitosano/SBE-β-CD/Quercetina apresentaram uma morfologia regular e esférica. Já para o caso dos sistemas de entrega de SBE-β-CD/Quercetina foi possível verificar que a morfologia era irregular e não esférica. Além disso, foram também realizadas espectroscopia de infravermelhos por transformada de Fourier (FTIR) e espectroscopia de UV/vis onde foi possível verificar a presença de todos os compostos e as interações entre eles. Para os sistemas compostos por SBE-β-CD foi também possível verificar que a quercetina se encontrava completamente aprisionada dentro dos complexos de inclusão, não sendo visível os picos característicos da mesma nos espetros FTIR.

Para os melhores rácios de cada tipo de sistema foram realizados ensaios de viabilidade celular em células HeLa (HPV positivas), onde os resultados mais promissores foram observados para os sistemas de entrega de Quitosano/SBE-β-CD/Quercetina. Este tipo de sistema de entrega mostrou uma redução na concentração média inibitória (IC_{50}) de 59,84 μM para 43,55 μM durante 48h de incubação, quando comparado com a quercetina livre.

Desta forma, os resultados indicaram que existe um aumento do efeito terapêutico após o encapsulamento da quercetina com sistemas de entrega de Quitosano/SBE-β-CD/Quercetina, representando assim um passo em frente na conceção/desenvolvimento de sistemas de entrega baseados em flavonoides para aplicações de terapia do cancro do colo do útero.

Palavras-chave

Cancro do colo do útero; HPV; flavonoides; sistemas de entrega; quercetina.

Abstract

Human papillomavirus (HPV) is the main causative agent for the development of cervical cancer, the fourth most common cancer in women worldwide. Overexpression of HPV oncoproteins E6 and E7 are present on this type of cancer, disrupting the cell cycle regulation and proliferation through the involvement of tumor suppressor proteins p53 and pRb, respectively.

Although preventive anti-HPV vaccines already exist, therapies for this type of cancer are still under development in order to find an effective cure for this type of cancer. Flavonoids have shown a high potential in such therapy, offering an effective and low-cost method that enables their use in less developed countries and where health care is poorer.

Quercetin is the main flavonoid in therapeutic uses presenting high anticancer properties, showing particular prominence in cervical cancer therapy due to the fact that it potentiates E6 oncoprotein inhibition, thereby increasing p53 expression and thereby inducing apoptosis. However, quercetin use is limited due to its insolubility in aqueous medium and its low stability. Thus, quercetin low bioavailability limits its application in cancer therapies.

Thus, this master thesis aims to develop quercetin-loaded delivery systems to enhance its bioavailability and effect in HPV positive cells.

Three types of systems were formulated and characterized, one composed of sulfobutyl ether β-Cyclodextrin (SBE-β-CD) and the other two were chitosan-based, one conjugated with tripolyphosphate (TPP) and other with SBE-β-CD. SBE-β-CD/Quercetin delivery systems had a size of 2468.33 nm, a polydispersity Index (PdI) of 0.123, a zeta potential of -21.03 mV and an encapsulation efficiency of approximately 100%. The Chitosan/TPP/Quercetin delivery systems showed a size of 325.1 nm, a PdI of 0.371, a zeta potential of +16.6 mV and an encapsulation efficiency of 10.80%. Finally, Chitosan/SBE-β-CD/Quercetin delivery systems presented a size of 272.07 nm, a PdI of 0.287, a zeta potential of +38.0 mV and an encapsulation rate of approximately 100%.

Scanning electron microscopy (SEM) was performed for all delivery systems, being possible to verify that Chitosan/TPP/Quercetin and Chitosan/SBE-β-CD/Quercetin systems presented a regular and spherical morphology. Furthermore, fourier transform infrared spectroscopy (FTIR) and UV/vis spectra were also obtained and it was possible to verify the presence of all compounds and the interactions between them, and, for the systems composed by SBE-β-CD it was also possible to verify that it was completely trapped inside the inclusion complexes.

Cell viability assays were performed in HeLa cells (HPV positive) for each type of formulated system, with the most promising results being seen for the Chitosan/SBE-β-CD/Quercetin delivery systems. This type of delivery system showed a reduction in half inhibitory concentration (IC_{50}) from 59.84 μM to 43.55 μM for 48 h of incubation when compared with free quercetin.

In this manner, the results indicated that there is an increased therapeutic effect after encapsulation with Chitosan/SBE-β-CD/Quercetin systems, thus representing a step forward in the design/development of flavonoids-based delivery systems for cervical cancer therapy applications.

Keywords

Cervical cancer; HPV; flavonoids; delivery systems; quercetin.

Index

List of Figures

List of Tables

List of Abbreviations

BSA	Bovine serum albumine
CIS	Carcinoma in situ
DLS	Dynamic Light Scattering
DMEM-F12	Dulbecco's Modified Eagle's Medium/Ham's F-12 nutrient mixture
DMSO	Dimethyl sulfoxide
DNA	Deoxyribonucleic acid
DR	Drug release
E	Early region
E6AP	E6-associated protein
EE	Encapsulation efficiency
FTIR	Fourier transform infrared spectroscopy
GLOBOCAN	Global Cancer Observatory
HMW	High molecular weight
HPLC	High-performance liquid chromatography
HPV	Human papilloma virus
IC50	Half inhibitory concentration
L	Late region
LCR	Late control region
MMPs	Matrix metalloproteinases
MTT	3-(4,5-dimethylthiazol-2-yl)-2,5-diphenyltetrazolium bromide
NIC	Cervical intraepithelial neoplasia
NLCs	Nanostructured lipid carriers
ORF	Open reading frames
PBS	Phosphate-buffered saline
PdI	Polydispersity index
PEG	Polyethylene glycol
pRb	Retinoblastoma protein
RNA	Ribonucleic acid
ROS	Reactive oxygen species
SBE-β-CD	Sulfobutyl ether beta-cyclodextrin
SEM	Scanning electron microscopy
SLNs	Solid lipid nanoparticles
TPP	Tripolyphosphate
UV	Ultraviolet
v/v	Volume/volume
VR	Viability reduction
ZP	Zeta potential

List of Scientific Publications

Review: Ferreira, M.; Costa, D.; Sousa, Â. Flavonoids-Based Delivery Systems towards Cancer Therapies. *Bioengineering* **2022**, *9*, doi:10.3390/bioengineering9050197 (Annex).

Book chapter: Eusébio, D.; Albuquerque, T.; Neves, A.R.; Faria R.; Ventura, C.; Ferreira, M.; Sousa, Â.; Costa, D.; Chapter 38: Drug delivery for bone tissue engineering; Advanced and Modern Approaches for Drug Delivery (under revision)

List of Scientific Communications

Oral communication: Ferreira, M.; Gomes, D.; Ventura, C.; Gonçalves, A.M; Passarinha, L.A.; Costa, D.; Sousa, Â.; Formulation of quercetin-loaded nanoparticles to improve cervical cancer therapy; **2022**; XVII International CICS-UBI Symposium, Covilhã, Portugal.

Chapter 1 – Introduction

1.1. Cancer

Cancer diseases are one of the main causes of death worldwide, being characterized by an uncontrolled and abnormal growth of cells. An initiating agent causes anomalies in the cell machinery or mutations in deoxyribonucleic acid (DNA), leading to an uncontrolled proliferation of these anormal cells and resulting in a tumor. These cells can also trigger metastases in other parts of the body after cancer progression. According to the Global Cancer Observatory (GLOBOCAN) database, it was estimated that 19.3 million new cases appeared, leading to approximately 10 million deaths in 2020 [1].

Worldwide, the highest cancer incidence rates are attributed to breast (11.7%), lung (11.4%) and colorectal (10.0%) cancer, corresponding to almost a third of the incidence rate and mortality worldwide, as shown in Figure 1. Regarding the mortality rate, lung cancer is the main responsible (18.0%), followed by colorectal cancer (9.4%) and liver cancer (8.3%), as presented in Figure 2. Breast cancer, despite being the type of cancer with the highest incidence rate, is in fifth position in terms of mortality (6.9%) due to the relatively favourable prognosis, especially in more developed countries that have better conditions in health care [1].

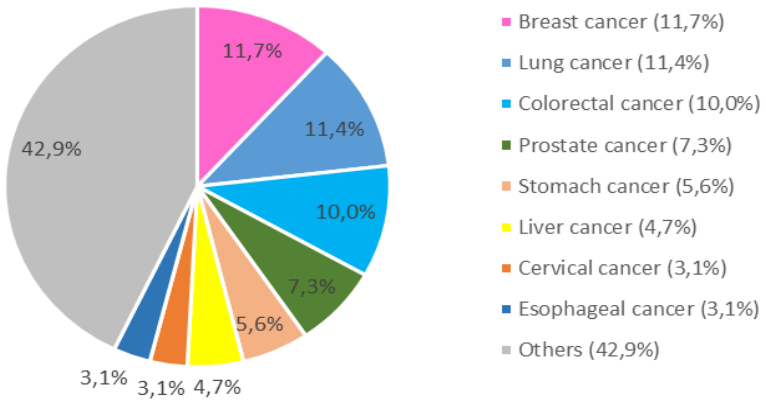

Figure 1: Estimated incidence rate of new cancer cases in 2020 (adapted from [1]).

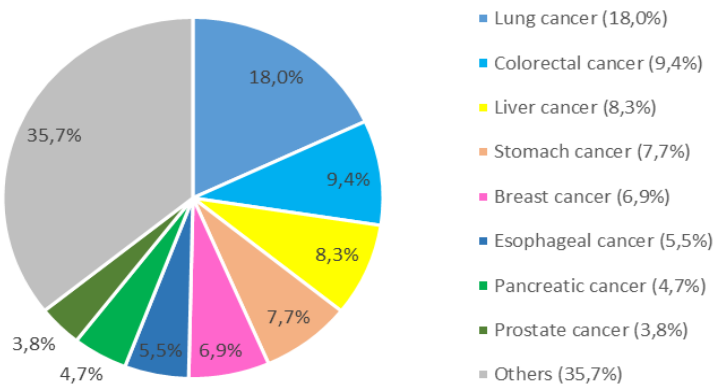

Figure 2: Estimated cancer mortality rate in 2020 (adapted from [1]).

The development of cancer diseases has been widely studied in recent decades and many causes have already been discovered as risk factors for its development. Risk factors such as age, genetic predisposition, ethnicity, environmental exposure, lifestyles (diet and physical activity, for example) are some of the risk factors already explored. Other types of risk factors are associated with infections by bacteria, parasites or viruses such as the human papilloma virus (HPV) that has some prominence in the development process of some cancers such as head, neck, vaginal, vulvar, penile, anal cancer and especially cervical cancer [2].

1.2. Cervical cancer

According to GLOBOCAN, cervical cancer is the fourth type of cancer with the highest incidence among women in the world (6.5%), as shown in Figure 3, being mainly associated with high-risk HPV subtypes, which represent between 79% and 100% of the cases [3,4].

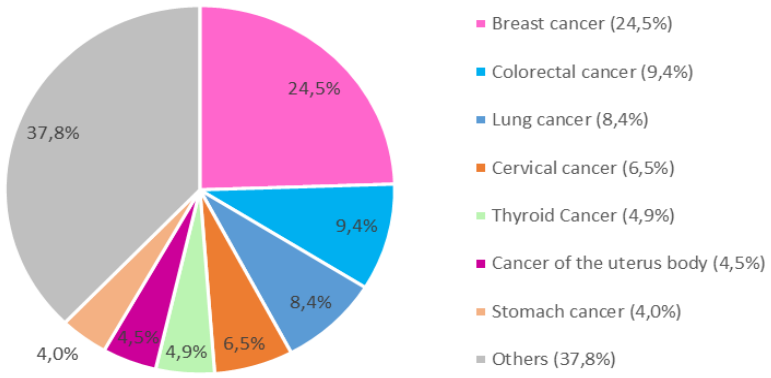

Figure 3: Estimated incidence rate of new cancer cases in women worldwide in 2020 (adapted from [3]).

The cervical cancer mortality rate is, like the incidence, the fourth most important (7.7%), representing a number of deaths of more than 340.000, in 2020 alone. The mortality rate in women worldwide is represented in Figure 4 [3].

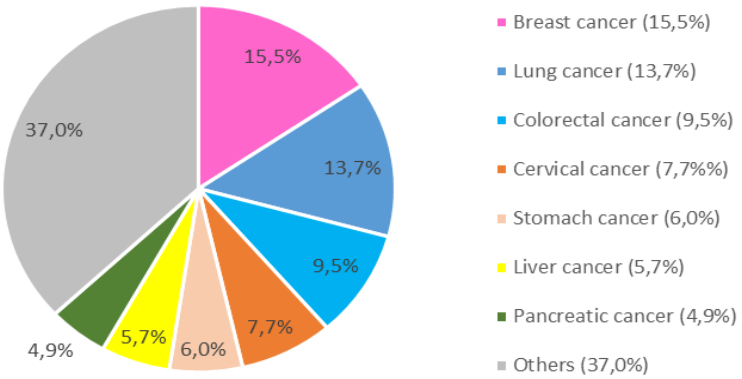

Figure 4: Estimated cancer mortality in women worldwide in 2020 (adapted from [3]).

However, these numbers are particularly noteworthy when we consider the estimates of incidence and mortality rates in less developed countries, where cervical cancer is the second leading cause of cancer in women (21.1%), only surpassed by breast cancer (28.3%), as can be shown in Figure 5 [5]. Together, these two types of cancer represent almost half of the new cases of cancer in these countries. The same tendency is also reflected in the mortality rate, where breast cancer appears in first (23.1%) followed immediately by the cervical cancer (22.1%), as represented in Figure 6 [5].

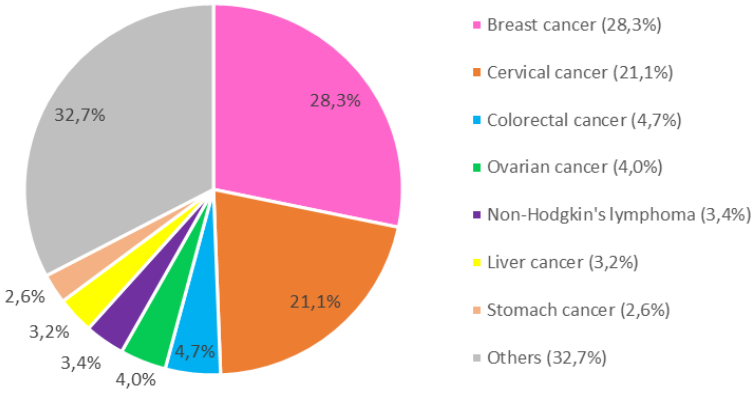

Figure 5: Estimated incidence rate of new cancer cases in women in least developed countries in 2020 (adapted from [5]).

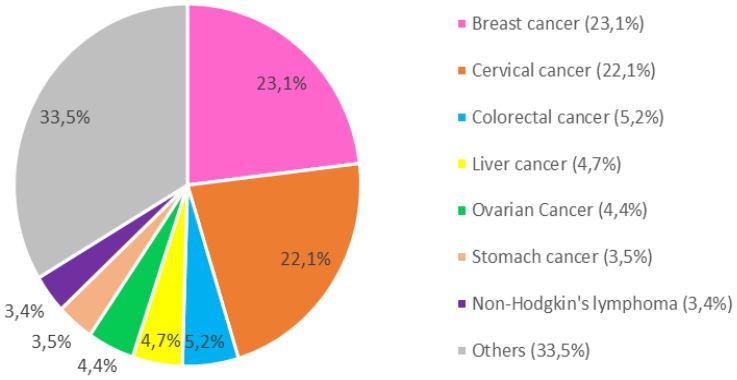

Figure 6: Estimated cancer mortality in women from least developed countries in 2020 (adapted from [5]).

The increase in the incidence and mortality of cervical cancer in less developed countries is mainly associated with the lack of health care compared to more developed countries, as well as the low distribution of anti-HPV vaccines [6].

1.3. Human papilloma virus

As mentioned before, the human papilloma virus is the main factor for the development of cervical cancer (being responsible for 79% to 100% of cases) [4]. HPV belongs to the *Papillomaviridae* family and has more than 200 different genotypes, which can be divided into 3 supergroups, summarized in Table 1. The Alpha group represents the one with the highest incidence and where all the sexually transmitted genotypes are found [7].

Table 1: HPV groups and diseases associated with each group (adapted from [7]).

Supergroup	Subgroup	Associated diseases
A	Alfa	They can infect oral sites where they are associated with benign papillomas. It causes mucosal lesions that progress to neoplasms and cancer.
B	Beta	It causes subclinical infections, but in immunosuppressed patients it can cause skin cancers at the site of infection.
	Gama	Causes skin warts.
E	Mu	It causes skin and plantar warts.
	Nu	

Regarding the genotypes that infect the mucous membranes, namely the *Alphapapillomaviruses*, they can also be classified according to their oncogenic potential, being distinguished into low-risk genotypes and high-risk genotypes, as summarized in Table 2 [8].

Table 2: HPV genotypes classified according to their oncogenic potential (Adapted from [8]).

HPV	Genotypes
Low-risk	6, 11, 40, 42, 43, 44, 54, 61, 70 ,72 e 81.
High-risk	16, 18, 31 ,33, 35, 39, 45, 51, 52, 56, 58, 59, 68, 73 e 82.

In the case of low-risk genotypes, they are mainly related to benign epithelial lesions, while, in the case of high-risk genotypes, these are mostly related to neoplasms and cancers [9,10].

Regarding their potential, 15 are classified as genotypes of high oncogenic potential, and the genotypes with the highest prevalence are HPV16 and HPV18, being responsible for 50-60% and 10-20% of cases of cervical cancer worldwide, respectively [11].

1.3.1. HPV genome

HPV is a virus with a high capacity to induce proliferative lesions in the skin and internal mucosa. Its genome is characterized by a double strand of circular DNA of

about 8000 base pairs, a non-enveloped icosahedral structure and a size of 50-55 nm in diameter [4].

This genome encodes a total of 8 open reading frames (ORF) and is divided into three regions: the early region (E), the late region (L) and the late control region (LCR) [12]. The HPV genome structure is represented in Figure 7.

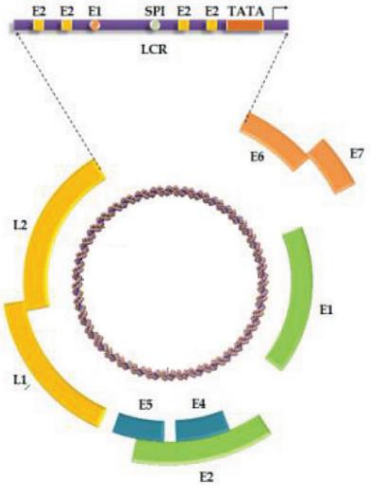

Figure 7: Human Papillomavirus genome structure (Adapted from [13]).

The early region is constituted by the genes E1, E2, E4, E5, E6 and E7 and is essential for the viral cycle and cell transformation. The late region encodes L1 and L2 proteins and is responsible for the formation of the capsid that protects the viral genome [14].

The late control region is a non-coding regulatory region located between E6 and L1 and contains the origin of replication and transcription factor binding sites, allowing to regulate the replication and transcription of genes that constitute the early and late regions [15].

All the function of HPV genes are summarized in Table 3.

Table 3: Functions of Human Papilloma Virus genes (Adapted from [14]).

Region		Gene	Function
Coding	Premature	E1	Responsible for viral replication and transcription.
		E2	Viral DNA replication and is an E6 and E7 transcriptional repressor.
		E4	It can bind to cytoskeletal proteins and break the cytoskeleton network, contributing to the deformation of infected cells.
		E5	It inhibits apoptosis and interacts with growth factor receptors.

		E6	It induces the degradation of the tumor suppressor protein p53, alters cell cycle regulation and leads to cell immortalization.
		E7	It binds to the retinoblastoma protein (pRb) tumor suppressor gene leading to its degradation, re-entry into the S phase of the cell cycle.
	Late	L1	It encodes the main viral capsid protein (55 kDa).
		L2	It encodes the viral capsid secondary protein (70 kDa).
Non-coding	Late control	LCR	Regulates viral replication and transcription.

1.3.2. HPV life cycle

HPV infection is transmitted by skin-to-skin contact, due to micro lesions in the basal layer of the epithelium [14].

After becoming infected, the early E1 and E2 proteins start to be expressed in the undifferentiated epithelial cells of the basal layer, regulating viral replication and further expression of viral early proteins [4]. At this stage, the viral replication cycle is completely conditional on the differentiation cycle of the infected cells, since the virus DNA only replicates when the DNA of the infected cells is replicated [14].

Therefore, after the differentiation of the infected basal cells, they will start to express E6 and E7 viral proteins, that will act as stimulators of cell proliferation, prolong the cell cycle progression and prevent apoptosis. The expression of these two oncoproteins occurs due to the absence of the E2 protein that are no longer expressed after integration of the DNA into the genome of the infected cells. Therefore, E2 absence leads to a higher expression of E6 and 7, thus enhancing the development of evil lesions [14]. At this time, the cells have a faster life cycle and divide more often, causing the infected cells to increase in number and replacing the normal ones.

The synthesis of L1 and L2 proteins occurs in the final phase of the cycle in the most superficial layers of the epithelium, forming the capsid and giving to the viral genome more protected [14].

Finally, the more differentiated cells produce virions that are released by keratinocytes, located more superficially, as they die [14].

The entire process that takes place from infection to the appearance of cancer is called carcinogenesis. It is a complex process with many stages, with genes associated with the transformation of normal cells into cancer cells in each of these stages of evolution, as well as the changes that the epithelial tissue undergoes over time, from the point at which it is normal epithelial tissue, progressing to cervical intraepithelial neoplasia (NIC) with a grade between 1 and 3, undergoing carcinoma in situ (CIS) and taking finally to the emergence of cervical cancer [14]. All processes are schematized in Figure 8.

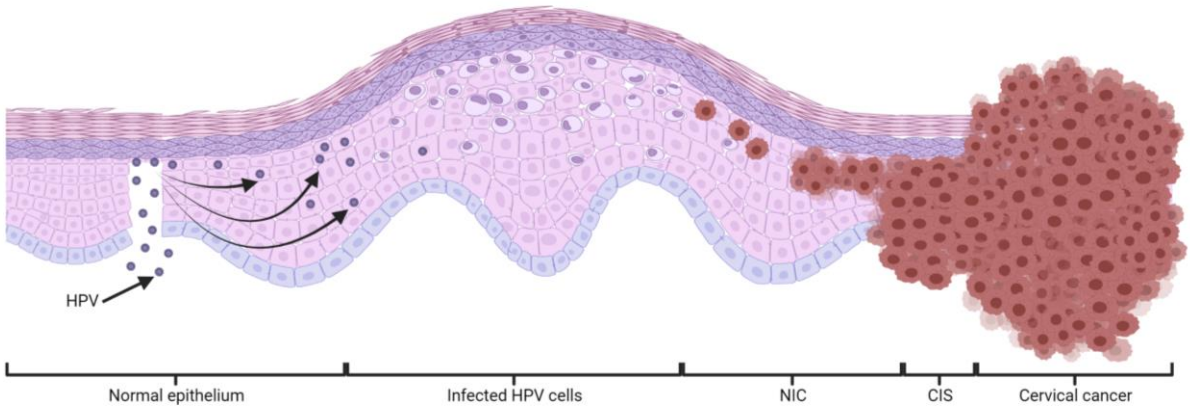

Figure 8: Schematic representation of HPV-mediated infection of the basal cells of the cervical epithelium in the course of time (Adapted from [16]).

1.3.3. E6 and E7 oncoproteins

The E6 and E7 viral genes that are present in the HPV genome are transcribed in the infected cells, expressing the respective oncoproteins that emerge as the main oncogenic power [11]. E6 and E7 oncoproteins have the ability to bind to the tumour suppressor proteins p53 and pRb, respectively, stimulating their degradation.

E6 oncoprotein consists of approximately 150-160 amino acids with 18 kDa, having four Cys-X-X-Cys motifs that form two zinc fingers [17]. This oncoprotein forms a complex with the E6-associated protein (E6AP), a ubiquitin ligase required for the interaction with p53 protein [18]. Thus, the formation of this trimeric E6-E6AP-p53 complex enhances the degradation of the p53 tumour suppressor protein via ubiquitination. In this way, the reduction in the p53 activity favours DNA replication in infected cells and enhances cell survival, inhibiting apoptosis and thus potentiating carcinogenesis [4]. Furthermore, E6 also has an equal capacity to degrade other cellular

proteins present in the signalling cascade for apoptosis, such as Bak, FADD and procaspase 8, favouring further inhibition of apoptosis [4,18].

On the other hand, the E7 oncoprotein is formed by 98 amino acids and has a C-terminal zinc-binding domain that plays an essential role in oncoprotein activity [19]. Furthermore, and as previously mentioned, the E7 oncoprotein has a high affinity for pRb, thus potentiating the inhibition of the activity of this tumour suppressor protein [4]. Under normal physiological conditions and at specific times in the cell cycle, namely during the transition to the S phase, the pRb protein forms complexes with transcription factors of the E2F family [4,18]. These complexes negatively regulate cell growth by suppressing transcription of E2F-dependent genes. In the case of an HPV infection, there is the production of the E7 oncoprotein which, by binding with the pRb tumour suppressor protein, causes it to lose its ability to regulate the E2F family transcription factors, resulting in continued DNA replication and progression of the viral cycle.

The combined action of E6 and E7 oncoproteins results in a synergistic effect, leading to increased uncontrolled cell proliferation and other processes involving carcinogenesis, represented in figure 9 [20].

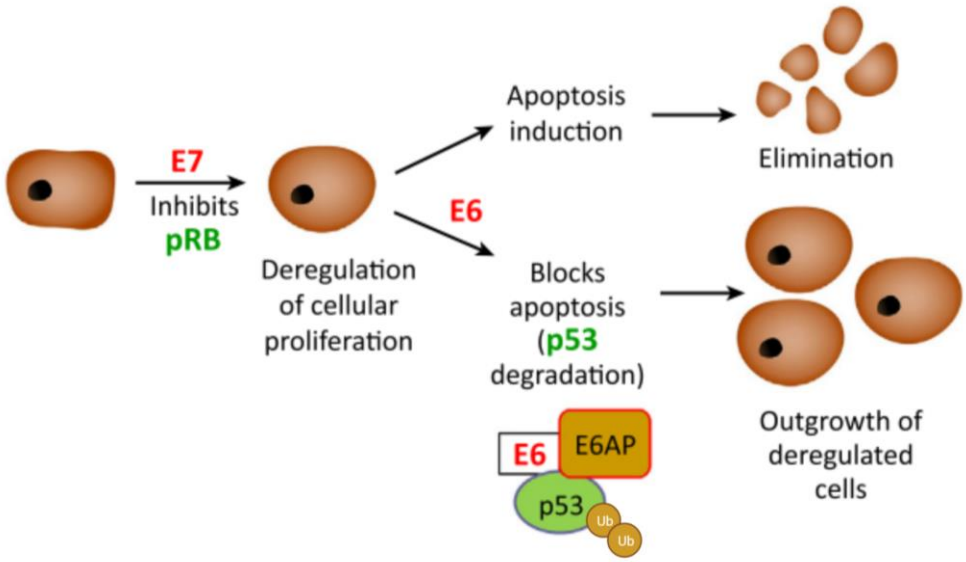

Figure 9: Synergetic effect of E6 and E7 oncoproteins in HPV infected cells (adapted from [20]).

1.4. Current therapies

Cancer remains one of the deadliest diseases worldwide. Current treatments include surgery, radiation, and chemotherapy. However, these treatments have a very limited success rate, resulting only in some situations against localised early-stage tumours, and rarely being effective in more advanced stages or in case of metastases formation [4]. Therefore, the development of new therapeutic strategies that induce long-lasting protection and that specifically eliminate cancer cells, such as DNA vaccines, gene therapy and drugs with a high anticancer capacity, is fundamental.

At this moment, three commercial prophylactic vaccines are available and offer protection against the main high-risk HPV types. The three preventive vaccines currently available and the respective types of HPV that each can prevent are summarised in Table 4.

Table 4: Preventive vaccines already available for HPV infection.

Preventive vaccine	HPV types
Cervarix	16 and 18
Gardasil	6, 11, 16 and 18
Gardasil 9	6, 11, 16, 18, 31, 33, 45, 52 and 58

However, as described above, in less developed countries and where healthcare is more limited, these vaccines are not administered to the entire population, which results in the incidence and mortality rate of this type of cancer remaining very high. In this sense, new therapies are being studied in order to find an effective, specific and cheaper way to prevent or treat this type of cancer [18].

These therapies currently under study may involve the use of DNA- or ribonucleic acid (RNA)-based gene therapies, which have shown great potential, but are expensive and limit the possibility of using them in less developed countries. In this context, other therapies such as the use of natural compounds have been studied due to their low cost and low toxicity when compared with other molecules [21]. Some flavonoids are among the natural compounds that have a high anticancer capacity, having a special relevance in the treatment of cervical cancer due to their ability to inhibit E6 oncoprotein, as it is the case of quercetin [21,22].

1.5. Flavonoids

Flavonoids are a family of phenolic compounds present in plants, fruits and vegetables which are characterized by having a carbon skeleton base of C6-C3-C6. These compounds are widely used as dietary supplements and are of considerable scientific relevance, being reported to be antidiabetic [23], antioxidant [24], anti-inflammatory [25], antimicrobial [26], antiviral [26] and anticancer agents [27].

Presently, the major focus relies on the use of flavonoids in anticancer therapies, of which the use of epigallocatechin-3-gallate, quercetin, genistein, luteolin, apigenin, silibinin, naringenin and kaempferol been already reported [28,29]. Such flavonoids have been demonstrated to have significant anticancer capacity, notably through mechanisms such as inactivation of the carcinogen, induction of cytotoxic activity, increased antioxidant activity, inhibition of angiogenesis, induction of apoptosis, reduction of oxidative stress, enhancement of DNA repair processes and inhibition of cell proliferation [28,29]. All these mechanisms are summarized in Figure 10.

Figure 10: Schematic representation of the main mechanisms responsible for the anticancer potential of flavonoids (adapted from [16]).

Although all the mechanisms that contribute to the anticarcinogenic potential of flavonoids have been reported, the pathway leading to each one of them is yet to be

fully understood. Thus, there are still studies being carried out to fully unlock the mechanisms of action of flavonoids in an effort to improve the flavonoid's effects and reduce their limitations. Reduction of reactive oxygen species (ROS) and induction of apoptosis via death receptors, for instance, are considered the two main mechanisms of action, and are present in the majority of flavonoids [30].

ROS reduction is a main mechanism of flavonoid's action, being accountable for the inhibition of cell proliferation and a subsequent decline in tumour growth [30]. The ROS are widely reported to be responsible for causing irreversible DNA damage, thereby resulting in the creation of cancer cells and their uncontrolled growth. In addition, they also produce proto-oncogenes that can induce further cell growth [30,31]. The activity of flavonoids allows a diminution of ROS and, in consequence, a reduction in cell proliferation and proto-oncogenes, thus reducing the risk of advancement to more dangerous stages of cancer [31]. This mechanism is summarized in Figure 11.

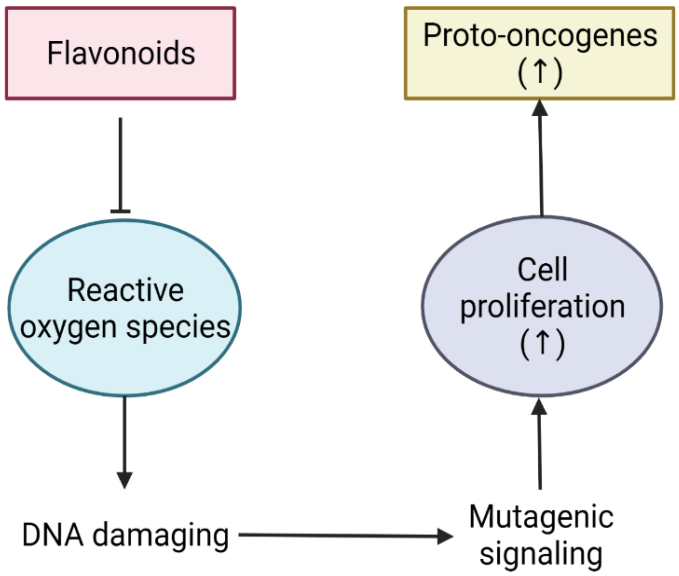

Figure 11: Scheme illustrating the flavonoid action on the reactive oxygen species (ROS) pathway (adapted from [16]).

The induction of apoptosis is other of the major mechanisms of action, being accountable for the triggering of death receptors, and the activation of the proapoptotic members Bax and Bak, as summarized in Figure 12 [30]. Bax, Bak and Bid are apoptosis regulatory proteins that are capable of releasing cytochrome c into mitochondria [30]. Such release leads to caspases activation, namely caspase 9 and 3, causing the cells to enter into apoptosis [31].

Furthermore, the flavonoids are capable of activate death receptors that will both stimulate caspase 8 as well as the proapoptotic member Bid, that in turn permits the release of cytochrome c [31]. Therefore, in either of such pathways, the cells will always enter into apoptosis, thus promoting tumour reduction.

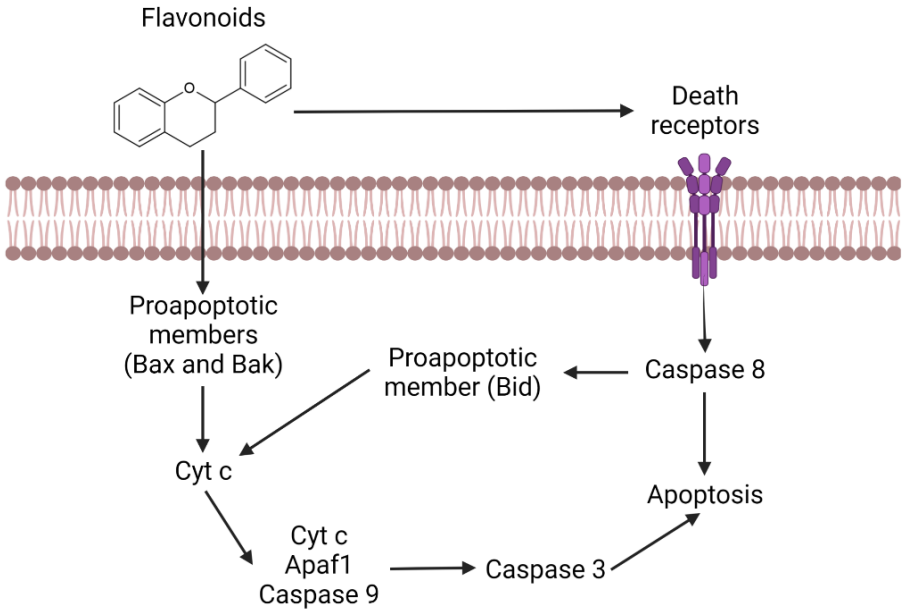

Figure 12: Representation of the apoptotic pathway mediated by flavonoids (adapted from [16]).

The action of flavonoids can be significantly different depending on the type of flavonoid, with some exhibiting differences in antioxidant power, the ability to reduce ROS, and the induction of apoptosis, among others [32].

Flavonoids have another important mechanism of action against cervical cancer, specifically through the suppression of the E6 oncoprotein [33]. As mentioned previously, the inhibition of this oncoprotein leads to an increase in p53 levels, thereby resulting in an increase in the apoptosis induction [33]. This mechanism constitutes a specific and improved action of flavonoids in the cervical cancer in comparison with other types of cancer, increasing its applications.

In addition, the use of flavonoids as adjuvants to chemotherapeutic agents, like doxorubicin or paclitaxel, has also undergone intensive studies [34–37]. In this type of therapy, its application promotes the intracellular accumulation of the drug in cancer cells and has led to a significant reduction in the proliferation/growth of cancer cells. Furthermore, they have contributed to reduce toxicity in healthy cells, thereby decreasing the side effects. The joint action of flavonoids and anticancer drugs then overcomes one of the main restrictions of chemotherapy and increases the anticancer action of the drug at a lower concentration [34–37].

1.5.1. Flavonoids subgroups

As described before, flavonoids are a class of polyphenols which can be classified in accordance with their biosynthetic origin, as well as based on the aromatic ring binding site and the degree of oxidation and saturation of carbons that are present between these two rings [38].

Currently, flavonoids can be divided into various subgroups. The main subgroups are summarized in Figure 13 and the characteristics and main actives of each subgroup are further described in the points below.

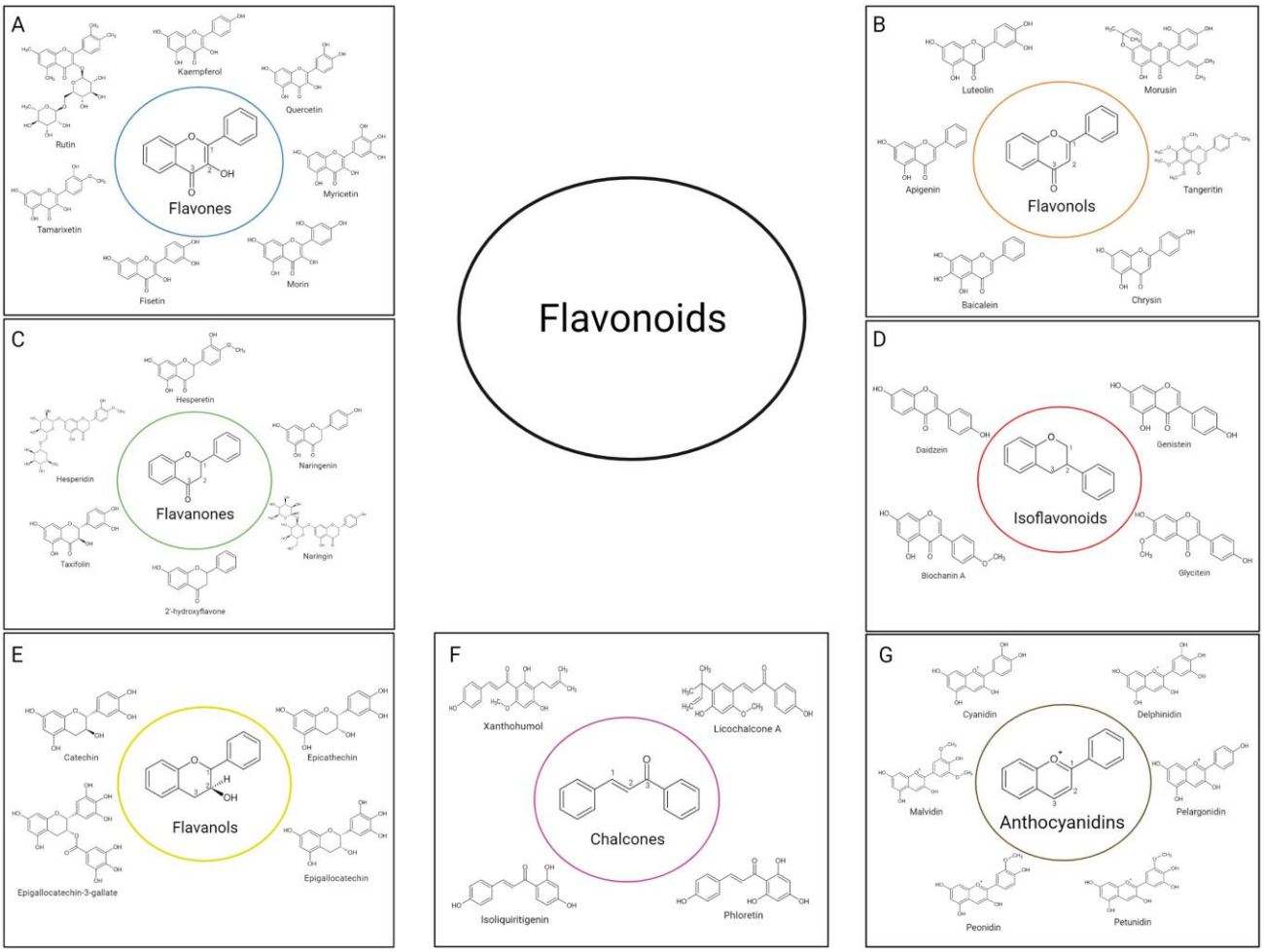

Figure 13: Classification of flavonoids: (**A**) flavones, (**B**) flavonols, (**C**) flavanones, (**D**) isoflavonoids, (**E**) flavanols, (**F**) chalcones, (**G**) anthocyanidins (adapted from [16]).

1.5.1.1. Flavones

Flavones are distinguished by a double bond across the carbons represented by the numbers 1 and 2 and a ketone group on the carbon represented by the number 3 in Figure 13.A [39]. The scientifically most prominent flavones are luteolin, morusin, tangeritin, chrysin, baicalein and apigenin, which are also shown in Figure 13.A [39]. In nature, flavones are typically present in their glycosylated form and can be obtained from fruits, leaves and flowers. Parsley, red pepper, mint, celery, camomile, orange, honey and ginkgo biloba are the main sources of this flavonoid group [40]. Flavones are chemically used to control the interactions of insects and micro-organisms with the plants and thereby protect them. They also belong to the group of non-essential nutrients and are largely applied in the food industry for this reason [30].

Flavones have several benefits to humans, such as the ability to decrease ROS production by inhibiting the enzyme xanthine oxidase, thereby suppressing efflux pumps and inducing apoptosis. Moreover, the flavones may also interact with oestrogen receptors, preventing them from losing their shape and thus binding to carcinogenic co-activators [32,38].

1.5.1.2. Flavonols

Flavonols mainly distinguish themselves from flavones essentially by a higher oxidation state, with this group's base skeleton containing an -OH group on carbon shown by the number 2 in Figure 13.B. Being the most representative group in nature, flavonols can be found in fruits and vegetables such as bananas, apples, onions, broccoli and grapes, as well as in red wine and teas such as black and green tea [38]. The most relevant and prominent flavonol in both scientific and therapeutic studies is quercetin, although there are other flavonols with high scientific interest, such as kaempferol, rutin, myricetin, morin, fisetin and tamarixetin.

In the natural environment, flavonols are believed to play a major role in plant growth and development, as well as in resistance to ultraviolet (UV) radiation and insects [30]. Flavonols play an important role in human health due to their antioxidant, antimicrobial, anti-inflammatory, cardiovascular and anticancer activities. Quercetin represents the most clinically studied flavonol and its anti-cancer role has been scientifically demonstrated, particularly its inhibitory action against the growth of cancer cells. It avoids metastasis through inhibiting the secretion of matrix

metalloproteinases (MMPs), preventing epigenetic alterations, stopping progression in the cell cycle and increasing apoptosis of cancerous cells, avoiding oxidative stress and inhibiting angiogenesis [30,34,41–43].

Furthermore, and as previously mentioned, quercetin also has the important action of increasing p53 levels by suppressing the action of E6 oncoprotein [33]. The delivery of this flavonoid to HPV-positive cells leads to its binding to the E6 oncoprotein, thereby blocking the ability of E6 to link to E6AP, thus preventing its function [41]. As such, the expression levels of p53 remain high, thus potentiating apoptosis. In addition, quercetin also increases the expression levels of Bax and p21, further stimulating apoptosis [41].

1.5.1.3. Flavanones

Flavanones are defined by the fact that they contain saturated and deoxidised carbons as indicated by the numbers 1 and 2 in Figure 13.C. They are the primary product of the flavonoid biosynthesis pathway and the highest reactive flavonoid group. They are found in nature mainly in the skin of fruits, in seeds, in the bark and in flowers of most plants [38].

Hesperidin, hesperetin, naringenin, naringin, 2'-hydroxyflavone and taxifolin are the main flavanones and their chemical structure are also represented in Figure 13. C. Similarly to flavonols, flavanones also possess the ability to suppress the expression of MMPs, thereby decreasing their tissue invasiveness and the development of metastases [44]. Furthermore, flavanones also have antioxidant and anti-inflammatory properties [39]

1.5.1.4. Isoflavonoids

Isoflavonoids can be found in plants of the *Fabaceae* family, in particular soybeans, red cover and chickpeas, in which they are found as a secondary metabolite. They have an essential role of protecting the plant from attacks by pathogenic micro-organisms. Structurally, this flavonoids group is distinguished among the other groups due to the phenol group attached to the carbon, shown with the number 2, rather than being linked to the carbon shown at number 1 in Figure 13.D [32,45]. The isoflavonoids may be present in both their glycosylated and aglycosylated form (the aglycone forms). The main isoflavonoids can also be seen in Figure 13.D, specifically Daidzein, Genistein,

Glycitein and Biochanin A, which may also show up in glycosylated forms, namely *β-glycisudem, 6"-o-malonyl-glycoside* and *6"-o-acetyl-glycoside* [46].

Their therapeutic role in humans has been the subject of extensive studies and they have been found to be useful in the prevention of diseases like osteoporosis in women, diabetes, Kawasaki syndrome, Alzheimer's and heart disease. Moreover, isoflavonoids have also antioxidant capacity due to their ability to give hydrogen atoms from the groups attached to the benzyl ring, as well as through their ability to enable and express the antioxidant enzymes catalase, glutathione and superoxide dismutase [32,45]. Apart from these characteristics, its most important role in medical therapy is related to its anticancer capacity. Through their structural similarities to estrogens, isoflavones also have the capacity to bind to estrogen receptors, thus competing with them and reducing cancer-related estrogens. Accordingly, isoflavones are being widely used in therapies against breast cancer and other types of cancer [45].

1.5.1.5. Flavanols (Flavan-3-ols)

Flavanols, or Flavan-3-ols, have a structure with carbons fully saturated (shown by the numbers 1, 2 and 3), along with a hydroxyl group on the chiral carbon shown by the number 2 in the Figure 13.E [47]. The principal compounds in this group are catechin, epicatechin, epigallocatechin and epigallocatechin-3-gallate, and due to their name, this group can also be named catechins [47]. Flavanols are mainly present in tea leaves but they can also be found in chocolate, cocoa and apples [47]. For humans, flavanols have been described as able to inhibit the activity of digestive enzymes like α-amylase and α-glucosidase, leading to a reduction in blood glucose levels. Additionally, they have also been found to have an impact on blood pressure, lowering it and reducing the risk of cardiovascular disease. Furthermore, flavanols contain antioxidant, anti-depressant and anti-obesity properties. [32].

1.5.1.6. Chalcones

Regarding the chemical composition, chalcones represent the most distinguishable group of flavonoids because the carbons shown by numbers 1, 2 and 3 in Figure 13.F will not form a third ring between the two benzyl rings. Furthermore, chalcones have also a ketone group at the carbon indicated as number 3 in the same figure. This group of open-chain flavonoids can be easily found in plants of *Moraceae*, *Leguminosae* and *Compositae* families, being present in vegetables, fruits, grains, roots, flowers, teas and

wines [48]. The main flavonoids in this subgroup used for therapeutic purposes are licochalcone A, phloretin, xanthohumol and isoliquiritigenin [39].

In the natural environment, this group has the capability of protecting plants by neutralising ROS and thereby preventing molecular damage and attacks by microorganisms [49]. Chalcones have been reported to have various properties for medicinal purposes, including antifungal, anti-inflammatory, antibacterial, antiviral, anticancer, and neuroprotective capabilities, among others. Its ability to inhibit ROS is believed to be the main reason for all these therapeutic benefits [49].

1.5.1.7. Anthocyanidins

Being the only group with substantial aqueous solubility, anthocyanidins are typified by an unsaturated ring between the two benzyl rings, forming a flavylium cation, as can be seen in Figure 13.G [50]. The anthocyanidins are widely available in leaf, flower, vegetable and fruit pigments, being responsible for colours of blue, red and purple ranges. Along with its pigmentary properties, the inhibition of ROS and the physiological phase regulation of plant tissues are also a relevant part of their valences [51]. The main flavonoids present in this group are cyanidin, delphinidin, malvidin, pelargonidin, peonidin and petunidin, whose chemical structures are shown in Figure 13.G [51]. Across humans, anthocyanidins have the capacity to be neuroprotective, antioxidant, anti-diabetic, anti-obesity and anti-cancer, as well as being responsible for inhibiting cancerous growth [51].

1.6. Flavonoids bioavailability

Although all flavonoids have demonstrated a low toxicity, combined with the significant value in a therapeutic scenario already mentioned, nearly all groups display a very low bioavailability. This parameter changes greatly between compounds. Isoflavones, flavanones, quercetin glucosides and flavanols display the highest bioavailability across all flavonoid subgroups, despite being similarly weak for therapeutic applications [28,46]. Excluding anthocyanidins which display a significant aqueous solubility, their solubility in water is usually very low in all flavonoid groups and, therefore, their absorption is very limited by oral administration, thus reducing their bioavailability and therapeutic effect [50,52]. Additionally, flavonoids are considered to have low stability, easy degradation in extremely acidic medium, low intestinal permeability and

high metabolism, resulting in the bioavailability of flavonoids being considered very low [23].

In order to overcome such bioavailability constraints, several approaches based on delivery systems are being developed and focused on processes to enhance intestinal absorption, increase stability or modify the site of absorption [53–56]. Furthermore, the use of delivery systems improves flavonoid solubility, reduces gastrointestinal degradation, enhances absorption in the bloodstream, prevents renal clearance and also protects against secretion in the liver. Correspondingly, the study of flavonoid-based delivery systems has acquired high scientific relevance. [57].

1.7. Delivery systems

A variety of flavonoid-based delivery systems are under development for the anticancer therapy, particularly against cervical cancer. By taking into account these new types of delivery systems, it is possible to use lower flavonoids concentration as well as to use ligands that will efficiently deliver these systems to cancer cells, thus decreasing the risk of toxicity to healthy cells and increasing their therapeutic benefit. There are a variety of delivery systems to explore for the encapsulation of these drugs, depending on the material involved and the characteristics displayed by the drug. Accordingly, the delivery systems may be highly distinctive in nature, having the main groups summarized in Figure 14.

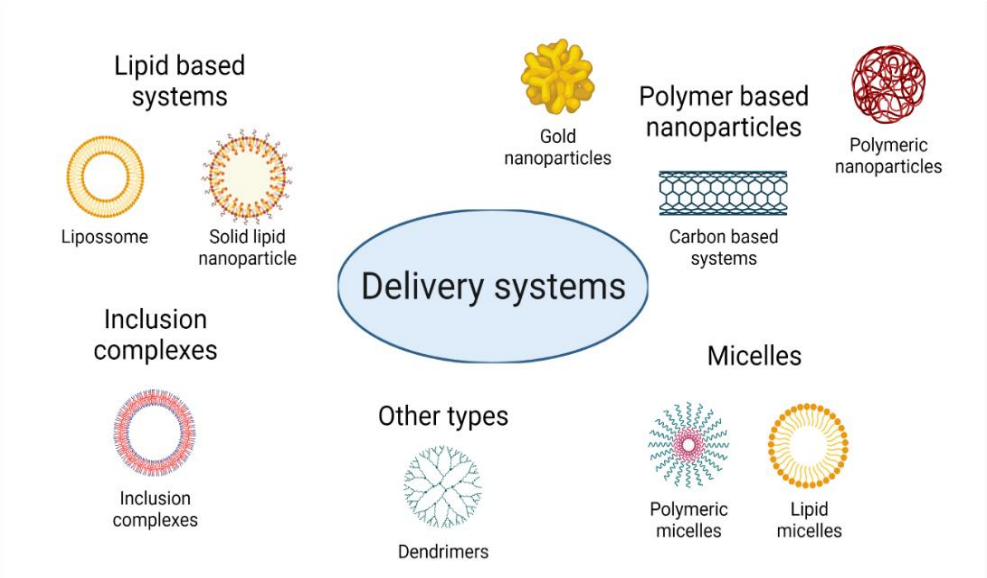

Figure 14: Principal types of delivery systems presently in development for the encapsulation of flavonoids (adapted from [16]).

The features of each different class of system and their constituent compounds are described in the following sections. The delivery systems are summarized in Table 5 and also indicates which are already being developed for *in vitro* (Hela cells) and *in vivo* (U14 cervical carcinoma) cervical cancer therapies.

Table 5: Delivery systems used in *in vitro* HeLa cells and *in vivo* U14 cervical carcinoma (adapted from [16]).

Type of Delivery System	Flavonoid	Constitution	Characteristics	Type of Study	Experimental Studies	References
Liposomes	Quercetin	Soybean phosphatidylcholine and cholesterol	Size: 143.1 nm EE[1]: 96.96%	*In vitro* and *in vivo*	IC_{50}[2]: 10–50 μM. DR [3]: 26.5% after 12h. Tumor decreases by about 50%.	[58]
		PEG[4], cholesterol and soybean phosphatidylcholine	Size: 171.3 nm EE: 81.25%	*In vitro* and *in vivo*	Toxicity: 10% IC_{50}: 3.033 μM after 48h. Tumor decreases from 1500 mm^3 to 500 mm^3.	[59]
		Egg-phosphatidylcholine, cholesterol and 2-distearoyl-sn-glycero-3-phosphoethanolamine-PEG 2000	Size: 109.79 nm. EE: superior to 80%	*In vitro*	IC_{50}: 185 μM, 40 μM and 14 μM were established after 24, 48 and 72h, respectively.	[60]
		Triglycerides, lecithin, PEG and acid folic	EE: 96.01%	*In vitro*	IC_{50}: 13 μM.	[61]
	Baicalein	Soybean phosphatidylcholine and cholesterol	Size: between 166.9 and 194.6 nm ZP[5]: between–18.23 and–30.73 mV EE: 44.3%	*In vitro*	Inhibition rate of 66.34%.	[62]
Nanoemulsion	Quercetin	Polyglyceryl-10 laurate, polyglycerol-6 monostearate and sucrose esters-11	Size: between 93 nm and 233 nm EE: 84.7%	*In vitro*	VR [6] to 90%.	[63]
Biopolymer	Quercetin	Chitosan and quinoline	Size: 174.8 nm EE: 77.2%	*In vitro*	IC_{50}: 10–14 ug/mL after 48h. DR: 69.3%–78.4% after 8h.	[64]
	Rutin and quercetin	Keratin and sodium dodecyl sulphate	Size: 55 nm ZP: –28.09 mV EE: 86.5%	*In vitro*	85% was released within 30h. VR up to 80%.	[65]

Biopolymer	Rutin	Fucoidan	Size: 221 nm	*In vitro*	IC_{50}: 20 µg/mL	[66]
	Naringenin	Silk fibroin	Size: between 148.4 and 180.1 nm ZP: between –30.5 and -39.1 mV EE: 21.81%	*In vitro*	IC_{50}: 250 µg/mL.	[67]
	Hesperidin	Gliadin coated with chitosan	Size: between 226.5 and 321.40 nm ZP: between–2.91 and +21.40 mV EE: between 73.10 and 80.11%	*In vitro*	IC_{50}: 16 ug/mL For blank nanoparticles IC_{50} of 159.33 µg/mL	[68]
Synthetic polymer	Genistein	Poly e-caprolactone and PEG 1000 succinate	Size: 181.83 nm ZP: –14.70 mV EE: 95.56%	*In vitro* and *in vivo*	IC_{50}: 24.3 ug/mL, 13.6 µg/mL and 5 µg/mL after 24, 48 and 72h, respectively. *In vivo* studies showed a reduction of tumour weight by about 4 times.	[69]
	Quercetin	Gelatin modified pluronics	Size: between 79.52 and 152.51 nm EE: 93.02%	*In vitro*	IC_{50}: 45.83 µM.	[70]
		PEG and poly lactide-*co*-glycolide	Size: between 143.1 and 153 nm EE: between 97.8% and 99%	*In vitro*	IC_{50}: 10 µM.	[71]
Inorganic polymer	Quercetin	Oxide nanoparticles functionalized with citric acid and α-cyclodextrin	Size: between 22.35 and 59.9 nm ZP: between–15.4 and +35.6 mV EE: higher than 75%	*In vitro*	VR: almost zero for nanoparticles with a drug concentration of 100 µg/mL.	[72]
	Phloretin	Gold nanoparticles	Size: 8 and 15 nm ZP: between–31.7 and–38.2 mV	*In vitro*	VR: 12.5% with a concentration of 4 mg/mL.	[73]
	Hesperetin, naringenin and apigenin	Copper complexes		*In vitro*	Inhibitory rate between 20 and 30%.	[74]
Inorganic polymer/ biopolymer	Quercetin	Copper nanoclusters with hydroxyapatite	Size: 36.2 nm ZP: –19.3 mV EE: 72%	*In vitro*	IC_{50}: 500 µM.	[75]
Inorganic/ synthetic polymer	Quercetin	Magnetic nanoparticles coated with poly citric acid and functionalized with folic acid and PEG	Size: between 10 and 49 nm EE: 80.3%	*In vitro*	VR: 25% with 100 µg/mL of quercetin. Toxicity: 0%	[76]

		Halloysites nanotubes functionalized with PEG	ZP: +37.44 mV	*In vitro*	VR: 30% for a drug concentration of 50 μg/mL. Toxicity: 10%.	[77]
	Quercetin and luteolin	Magnetic iron oxide nanoparticles modified with 3-aminopropyl triethoxysilane, folic acid and PEG	Size: between 8 and 20 nm	*In vitro*	VR: 20% and 40% with 100 μg/mL of quercetin and luteolin, respectively.	[78,79]
Micelles	Quercetin	Chondroitin sulfate and cholesterol	Size: between 124 and 237 nm EE: 30.6%	*In vitro*	VR: near to 80% for a drug concentration of 200 μg/mL.	[80]
Inclusion complex	Fisetin	Cyclosophoraose dimers	Showed 2.4 times more solubility of fisetin than β-cyclodextrin	*In vitro*	VR: 29% after an incubation of 24h with 100 μM of drug.	[81]
	Chrysin	β-cyclodextrin	Size: 458 nm ZP: −38.4 mV EE: 59.1%	*In vitro*	VR: 11.5% after 48h with 100 μM of drug.	[82]
Dendrimers	Baicalin	Poly amidoamine dendrimers modified with folic acid	Size: between 174.4 and 258.8 nm ZP: between−2.9 mV and−9.3 mV EE: between 53.5 and 91.9%	*In vitro*	VR: 40% after 48h with 25 μg/mL of baicalin.	[83]

[1] EE—Encapsulation efficiency (%). [2] IC_{50}—Half inhibitory drug concentration. [3] DR—Drug release. [4] PEG—Polyethylene glycol. [5] ZP—Zeta potential (mV). [6] VR—Viability reduction.

1.7.1. Lipid-Based delivery systems

Lipid-based delivery systems can be divided into three major groups: liposomes, solid lipid-based nanoparticles and emulsions, and within each of these groups there can be further divisions into subgroups [84].

1.7.1.1. Liposomes

Liposomes consist of a spherical vesicle usually formed by emulsifiers and a bioactive compound dissolved in an organic solvent. Generally they are made of with at least one lipid layer which permits them to be frequently employed for the encapsulation of both hydrophilic and hydrophobic drugs [58,85]. Liposomes are mainly composed of phospholipids and can also contain cholesterol and/or a hydrophilic polymer like polyethylene glycol (PEG). In such cases, they can be termed as stealth liposomes, since the junction with this kind of polymer extends the circulation time of liposomes,

thereby improving their efficiency. As regards liposomes formation with phospholipids and cholesterol, their use ensures structural and biological stability, giving origin to biocompatible transport systems with high encapsulation efficiency for all types of flavonoids, consistently higher than 80% and in several cases over 95%. [59]. Furthermore, liposome stability also decreases the capability of the systems to prevent the formation of aggregates, to be toxic for therapeutic use and to improve the capacity for a controlled release of encapsulated flavonoids. Nevertheless, there is still some physical and chemical instability that could lead to aggregation problems over time, as well as some drug degradation over the storage time. [59,60,86]. However, the utilization of this class of system also favours its size and polydispersity index (PdI), which vary from 100 to 200 nm and from 0.1 to 0.25, respectively. These favourable properties confer to these systems the ability to more easily move through the pores present in blood capillaries and accumulate in tumours, which usually present a greater number of pores in the blood capillaries that are surrounding them [59,60].

Both *in vitro* and *in vivo* trials demonstrated a high number of therapeutic benefits from applying liposomes, in particular through their high capacity to encapsulate flavonoids, resulting in increased therapeutic effect and reduced toxicity. The viability studies on cervical cancer cell lines (HeLa) shown that when the flavonoids are encapsulated in liposomes, it requires a lower concentration of flavonoids to obtain a half inhibitory concentration (IC_{50}) on cell viability studies, which can decrease from 200 μM in the case of free quercetin towards concentrations of nearly 100 μM after an incubation of 24 h, as demonstrated in Table 5. For extended incubation times, an IC_{50} can be achieved for concentrations of 14 μM by using liposomes made of triglycerides, lecithin, PEG and folic acid [60,61]. In addition, *in vivo* studies have shown that quercetin-loaded liposomes composed of PEG, cholesterol and soybean phosphate choline have induced an almost three times decrease in tumour size when compared with the delivery of free quercetin [58,61]. Other liposomes made up of soybean phosphatidylcholine and cholesterol showed a decrease in tumour volume of nearly 50%. [58]. For other cancers, the use of liposomes have been also investigated and equally showed a high encapsulation rate, a low toxicity and a high percentage of cell inhibition in *in vitro* studies [87–89]. Overall, a great range of emulsifiers have been already tested in anticancer therapies, in particular lecithin or PEG derivatives. In some cases, the chitosan coatings were explored in order to improve their bioavailability and stability in *in vivo* studies, thereby providing further possibilities to enhance the application of these systems in cervical cancer related studies.

1.7.1.2. Lipid-Based nanoparticles

A second widely investigated type of delivery system are solid lipid-based nanoparticles, which are described as being solid lipid systems that are formed at room temperature. These are divided between solid lipid nanoparticles (SLNs) and nanostructured lipid carriers (NLCs). The main distinguishing characteristics between SLNs and NLCs is the fact that SLNs form completely solid systems with a perfect crystal structure, compared to NLCs which have a non-ideal crystal structure that leads to the development of systems with both a solid and liquid zone, thereby increasing the drug load and reducing the water content [90–92]. Compared to liposomes, SLNs avoid the necessity of using organic solvents, therefore reducing their cytotoxicity, while still keeping a high capacity to encapsulate both the hydrophobic and hydrophilic drugs [86]. Thus, SLNs possess a high bioavailability, a low cost and an easy large-scale production and a high capacity to sustain a controlled release [86]. Regarding the composition, both SLNs and NLCs are principally made up of non-ionic surfactants such as Polysorbate 80®, Poloxamer 188, Tyloxa-pol, and occasionally lecithin or phosphatidylcholine, since their amphoteric character enhances the stability displayed by the system [74]. For NLC, there are liquid lipids that are used to make the liquid part of the system, such as oleic acid, olive oil, almond oil and cetiol®. [86]. Although all their advantages and their highly tolerance in *in vitro* and *in vivo* assays for being made up of natural components, the toxicity of the surfactants and the other excipients necessary for their production must be considered. Furthermore, there are still a potential risk of aggregation and recrystallisation present in this type of system [84,93].

The applications of SLNs and NCLs in cervical cancer related *in vitro* and *in vivo* assays are still not completely tested. Nevertheless, considering studies in others types of cancer, their use has proven that it was possible to achieve a high encapsulation rate (over 90%) and a drug load of over 10% and, in some cases, over 20%. [90,94–97]. It has also been proven a significant decrease in cell viability *in vitro* as well as a considerable reduction in tumour volume in *in vivo* studies [90,94–97]. These findings provide further support to the fact that the application of SLNs and NCLs in anticancer therapies against cervical cancer could be of special interest and should be further investigated.

1.7.1.3. Emulsion and nanoemulsions

Other than the latter types of delivery systems, emulsions and nanoemulsions can also be considered. This class takes advantage of the interactions between water and oils through an addition of an emulsifier such as polyglyceryl-10 laurate or PEG 660-stearate in order to form systems that promote the solubilization of flavonoids and improve their bioavailability [63,98]. Despite the fact that either emulsions or nanoemulsions have the disadvantage that they are not thermodynamically stable systems, disassociating over time, their implementation leads to a high rate of encapsulation of flavonoids, typically over 80% and a lower aggregation, while preventing gravitational separation [63]. Between emulsions and nanoemulsions, they are distinguished by their size, emulsions have a size exceeding 200 nm compared to nanoemulsions that have a size below 200 nm. According to the desired flavonoid delivery location, the usage of different emulsifier ratios may be tested so that the systems can feature a suitable size range to reach the targeted site and accumulate there with most easily [85,99].

Nanoemulsions made of soybean phosphatidylcholine and cholesterol were tested on cervical cancer cells and they only exhibited a 10% reduction of viability at a concentration of 200 μg/mL, although they have demonstrated a low toxicity, enhancing the possibility of further studies to increase their therapeutic capacity [63]. For other types of cancer, emulsions and nanoemulsions have shown similar physical characteristics regarding size, encapsulation rate and stability. Nevertheless, they also have a significant anticancer potential, as demonstrated by the significant diminution of viable cells. As an example, in melanoma cells, it was possible to obtain a considerable reduction in viability at concentrations of more than 50 μM of drug encapsulated in an emulsion of lecithin, castor oil and PEG 660-stearate while, in human colorectal carcinoma cells, it was possible to verify a decrease in viability of about 60% at concentrations of 25 μM of drug encapsulated in an emulsion of Labrasol®/Tween®, lecithin and Miglyol® 812 [98,100,101]. Thus, new formulations with novel emulsifiers as well as different ratios might be tested to further increase flavonoid encapsulation, enhance its anticancer effect, and improve the therapeutic effect. As such, major advancements can be made in the development of anticancer therapies based on such molecules.

1.7.2. Polymer-Based Nanoparticles

Polymer delivery systems have been the first and most widely applied/explored carriers for the encapsulation of flavonoids. Overall, such delivery systems are composed of nanoparticles and spherical walls with an exterior polymer and a core consisting of a hydrophobic surfactant that offers a high stability, solubility and bioavailability to the large part of the flavonoids [70,71,102]. To obtain a high final drug concentration, this type of delivery systems makes advantage of the dissolution of flavonoids in an organic compound, usually ethanol, which is subsequently removed by evaporation under vacuum, or by spraying or lyophilisation to reduce the cytotoxicity of the system [66,85]. The properties of these polymer-based nanoparticles can differ greatly depending on the type of polymer involved and can be classified based on their nature, being divided into natural, synthetic or conjugated with inorganic compounds [23,84].

1.7.2.1. Natural Polymers

Natural polymer-based systems, or also known as biopolymers, provide a wide range of systems, according to the components used in their formulation, and in the specific case of biopolymers, these are proteins and polysaccharides [84,85]. Such polymers guarantee a high degree of biocompatibility and biodegradability as well as a low cytotoxicity, making them widely used in *in vitro* and *in vivo* experiments [66–68]. Nonetheless, the use of such systems based exclusively on proteins or polysaccharides is uncommon. In many circumstances, a combination with other types of biopolymer or with a synthetic or inorganic-based polymer is often considered [68]. The use of a polysaccharide such as chitosan is very common, used in combination with a protein, a polysaccharide or another type of polymer. This approach was found to provide increased biocompatibility, biodegradability as well as stability to the systems. Furthermore, chitosan possesses mucoadhesive properties which contribute to improved delivery of systems to specific/mucosal targeted sites [64,68,103,104]. The conjugation of one biopolymer to another type of polymer is very common and leads to the formation of systems with improved performance for either *in vitro* or *in vivo* assays. Usually, they present sizes of under 200 nm and a high stability as well as controlled drug release, facilitating the delivery into the target cells. [64,65,68,105]. The polymeric natural systems containing polysaccharides appear as an important way of achieving greater bioavailability of systems, which are often applied alongside with other polymers or inclusion complexes [106–108].

The use of proteins such as bovine serum albumin (BSA), silk fibroin, keratin and gliadin were already experimented on cervical cancer cell lines. The only compound used without any other compound associated was silk fibroin, mainly because it was a copolymer with hydrophilic and hydrophobic blocks, making the flavonoids encapsulation easier and improving their stability [64–68,109]. Nevertheless, such a polymeric system made out of silk fibroin exhibited a comparatively large size relative to other systems, as well as a high IC_{50} of 250 μg/mL [67]. The use, in cervical cancer, of polysaccharides relied only on the conjugation of chitosan with another polymer, such as quinoline or gliadin, and the simple use of phacoidan, a polysaccharide with similar properties as chitosan, showed a relatively low IC_{50} of 20 μg/mL, despite the significantly high size of 221 nm [64,68]. Apart from the size reduction that occurs due to the conjugation of several types of polymers, this conjugation results also in a higher encapsulation rate, typically about 80%, higher than the 21.81% encapsulation rate observed with systems made of only a single protein [64–68,109].

1.7.2.2. Synthetic Polymers

Other type of polymer-based nanoparticles derive from synthetic polymers in which PEG is the more dominant, frequently utilized in combination with other types of systems in order to enhance the flavonoid solubility and provide an improved encapsulation rate [71,77]. In the PEG-based systems, encapsulation rate is usually high, generally higher than 90%, despite presenting a low degradation rate and low biocompatibility. [71,77,110]. Nevertheless, these negative effects may be significantly reduced through the formation of systems composed of a mixture of polymers in such a way that it is possible to implement them in *in vitro* and *in vivo* assays [23,71,84].

Studies have been performed *in vitro* and *in vivo* on anticancer therapies against cervical cancer, involving formulated PEG systems conjugated with poly lactide-coglycolide, poly e-caprolactone conjugated with PEG 1000 succinate, as well as pluronic systems modified with gelatin [69–71,77,109]. Systems for which PEG is not the main compound are discussed further in the section relating to this type of compound. Cell viability assays have demonstrated that it is possible to achieve low IC_{50} values near to 10 μM by using systems consisting only of synthetic polymers, in particular PEG and lactide-co-glycolide, on account of the high blood circulation time that these systems achieve. Furthermore, they have revealed a high capacity of conjugation with specific ligands, like folic acid, that actively promotes targeting of systems to cancer cells, since these cells have a higher amount of folic acid receptors in

comparison with healthy cells. [71]. The use of poly e-caprolactone and PEG 1000 succinate systems in *in vivo* studies have shown a four times higher tumor weight reduction compared to the administration of the drug in its free form [69].

1.7.2.3. Inorganic Compounds Conjugated With Polymers

Inorganic polymer-based delivery systems are one class that presents a greater diversity of applications, namely in drug delivery, tissue repair, hyperthermia and magnetic resonance imaging [76]. This type of carrier is mainly composed of gold, copper and even iron oxide nanoparticles which usually constitute delivery systems like nanoparticles or nanotubes [72–76]. Despite such systems have a high ability to aggregate, suffer oxidation, and display a low stability and biocompatibility, coating these systems with polymers such as PEG greatly exceeds those disadvantages, giving to these systems a site for flavonoids and ligands to attach to and thus making these systems viable [76].

Characterized by their very small sizes in comparison with other types of delivery systems, the inorganic polymeric carriers usually have sizes below 50 nm, as well as encapsulation rate ranging from 70 to 80%. [72–76]. Iron oxide magnetic nanoparticles coated with different polymers, such as BSA, α-cyclodextrin, citric acid, poly citric acid, PEG or 3- aminopropyl triethoxysilane have been explored to transfect HeLa cells [72,76,79]. Cell viability assays were highly variable according to the system used, and an IC50 of 10 μg/mL has been obtained for the process using nanoparticles based on iron oxide and BSA [109].

Polymeric carriers have been extensively investigated for other cancers as well, and various systems have been already tested to both encapsulate flavonoids and target them to cancer cells. Several polymers are highlighted below, namely PEG and chitosan, both mentioned above and presented in Table 5 [102,104,105,110,111]. Chitosan incorporation in system formation and conjugation with most different types of polymers has been experimented, including common conjugation with tripolyphosphate and functionalization with PEG or some type of inclusion complex, with the aim of improving the stability and solubility of the encapsulated flavonoids [42,103,112,113]. Besides the already described compounds, poly(lactic acid), poly(lactic-co-glycolic acid) and polycaprolactone have also been explored, and usually these systems are also conjugated with PEG or any of its derivatives in order to enhance flavonoids encapsulation [23,102,110,114–117]. *In vitro* assays mediated through these

systems have shown a reduction in cell viability that is similar to the one registered in *in vitro* assays in HeLa cells, suggesting that such a system is highly suitable for any cancer cell.

1.7.3. Micelles

Micelles are made up of amphiphilic molecules that, according to the polymeric or lipidic character of these molecules, can be classified as polymeric micelles or lipidic micelles [84,118,119]. The molecules that make up micelles offer a hydrophobic core capable of encapsulating therapeutic agents with a low solubility and an elevated hydrophobicity [118–120]. Therefore, micelles provide an ideal platform for the encapsulation of flavonoids, assuring a higher flavonoids stability as well as an adequate and more consistent release profile. [118–120]. On the other hand, the external part of micelles, consisting of the hydrophilic zone of the molecules, provides elevated protection and stability, resulting in increased bioavailability of the system [118]. In terms of advantages, such delivery systems are highly favoured by their small size, frequently below 100 nm, as well as their high thermodynamic stability, a high drug loading capacity, increased cellular uptake, and an easy large-scale production. Nevertheless, the formulations vary greatly depending on the ratios of the components considered, and an intensive study might be required until the ideal ratio is discovered [84,118,119].

In vitro experiments on cervical cancer cells showed that the delivery facilitated by micelles composed of chondroitin sulfate and cholesterol resulted in a 20% decrease in viability in a concentration of 200 μg/mL [80]. Furthermore, these micelles showed a relatively weak percentage of encapsulation, even presenting a very high percentage of drug loading, at respectively 30.6% and 23.4%. [80]. *In vitro* assays with other types of cancer, using micelles, showed better performances, namely an IC_{50} of 110 μM and 21.24 μM in breast and lung cancer cells were achieved, respectively [118–122]. In addition, these studies have also indicated improved physical conditions of formed micelles, with sizes less than 100 nm and an encapsulation efficiency greater than 80%.[118–122].

The performance of micelles in *in vivo* studies was also tested, and a reduction in size of more than three times when compared to using the flavonoid in its free form was observed [123]. Thus, the use of micelles for encapsulation and delivery of flavonoids needs to be further studied before their widespread use. The combination of

characteristics displayed by these systems should be optimized to increase the performance of each one as a delivery vector for targeted delivery, and this would certainly have repercussions on its therapeutic potential against cervical cancer.

1.7.4. Inclusion complexes

Inclusion complexes can be defined as delivery systems that are characterized by having a host molecule with ability to attach another molecule by using non-covalent forces. The flavonoids can be "bound" to such complexes because of their capability to form hydrophobic interactions with them [23,84,85,107]. The main advantage of the inclusion complexes is the fact that they have a cone shape that is open on both ends with an outer hydrophilic surface as well as an inner hydrophobic surface. Flavonoids can thereby be "trapped" within the internal cavity, which greatly confers support to the improvement of their solubility, stability, and bioavailability [107]. Nevertheless, inclusion complexes have some drawbacks, with a restricted encapsulation rate for larger flavonoids, such as glycosylated compounds. In addition, they usually exhibit a comparatively large size (exceeding 200 nm) which limits their utilization for *in vitro* and *in vivo* controlled-delivery studies [106,108,124–126]. Subsequently, because of its low versatility, and due to the fact that there are cheaper methods of flavonoid encapsulation, their use is somewhat constrained.

This delivery system group mainly is made up of cyclodextrins, of which β-cyclodextrins are the most common. They can be converted in order to modify their physical and chemical characteristics to form more appropriate systems depending on the delivery site [107,124,125]. β-cyclodextrins are capable of altering their characteristics through chemical modifications to become more negatively or positively charged or having a greater or lesser degree of substitution [107,124,125]. There are different types of β-cyclodextrins, with β-cyclodextrin, carboxymethyl-β-cyclodextrin, sulfobutyl ether-β-cyclodextrin and hydroxypropyl-β-cyclodextrin (the most scientifically used) [107,108,124,126,127]. Cyclodextrins can also be combined with other polymers, such as chitosan, in order to increase both their stability, decrease their size and improve their bioavailability [107,108,127]. Additionally, the conjugation with biotin is also quite common since its receptors are highly expressed on cancer cells, which can contribute to effectively targeting cancer cells [126]. Other delivery systems based on inclusion complexes are tested for flavonoid encapsulation including α-cyclodextrins, γ-cyclodextrins and β-lactoglobulins [72,128,129].

In vitro studies on HeLa cells showed a reduction in viability to 11.5% after an incubation period of 48h, utilizing inclusion complexes consisting of β-cyclodextrin with a concentration of chrysin of 100 μM [82]. In other cancer-related studies, a major reduction in cell viability was also observed in comparison to the use of flavonoids in free form [82,124,126,130]. Thus, while it is important to be aware of the disadvantages already listed, the application of inclusion complexes for loading/encapsulation and delivery of flavonoids can be considered and investigated, as they easily promote solubilization of flavonoids in aqueous solutions, in which most of them cannot be dissolved.

1.7.5. Other types of Delivery systems

Alternative delivery systems could also appear as an alternative for encapsulation and targeting of flavonoids to cancer cells. Among the most promising carriers, dendrimers, for example, appear to be one of the most attractive.

Dendrimers are a group composed by polymeric materials which have a complex branched structure containing numerous functional groups and an interior cavity which allows the encapsulation of drugs, like flavonoids [76,131]. Poly(amidoamine) dendrimers are the most common and principal type of dendrimers studied, being already used in *in vitro* assays in several types of cancer and presenting remarkable results, such as a reduction of viability in HeLa cells down to 40% by using a concentration of baicalin flavonoids of 25 μg/mL [76,83].

Nevertheless, their applications are still limited because of the toxicity they present. Some approaches like PEG conjugation have been considered in order to minimize such effect and provide a stronger association with specific ligands [131,132]. For the future, new strategies to ensure higher stability and bioavailability of these systems have yet to be investigated to improve its effect on flavonoid encapsulation and subsequent delivery to target cells.

1.8. Chitosan

As previously mentioned, chitosan is a natural polysaccharide which is derived from the deacetylation of chitin, whose chemical structure is shown in Figure 15 [103]. Such a polymer has been extensively used for the formulation of delivery systems due to its

high biocompatibility and biodegradability, as well as having a low toxicity, a high mucoadhesive ability and also a cationic nature [112,133–135].

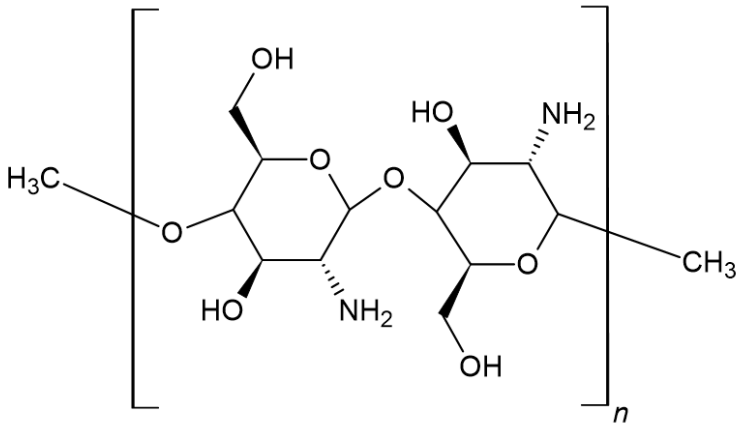

Figure 15: Chemical structure of chitosan.

The cationic nature of chitosan allows its conjugation with anionic compounds, enabling the connection of the positive charges of chitosan with the negative charges of another compound, such as tripolyphosphate (TPP) or sulfobutyl-ether-β-cyclodextrin [52,108,112]. Depending on the type and delivery site of systems, as well as the drug to be encapsulated, several parameters of the chitosan can be modified, namely the molecular weight, the degree of deacetylation and the formulation method that is chosen. Regarding their molecular weight, the use of chitosan with a high molecular weight, usually higher than 200 kDa, promotes the creation of systems with larger sizes, thereby allowing the encapsulation of bigger drugs [112,113]. On the other hand, when considering low molecular weight chitosan, normally smaller than 150 kDa, the systems have smaller sizes, which permits the encapsulation of smaller molecules, being for this reason widely used for the encapsulation of DNA vectors [136,137].

Likewise, the degree of deacetylation allows the presence of more or less amine groups, thereby potentially altering the ratios between amine and phosphate groups that are present in the system due to TPP or other type of crosslinker, leading to a change in the systems charge and facilitating cellular internalization. Also, the use of different formulation methods provides the possibility of altering the ratios between amine and phosphate groups on the surface of the delivery systems, as well as a change in their morphology and size. Thus, the use of chitosan conjugated with other types of system offers a high versatility, allowing the encapsulation of various types of drugs, namely of flavonoids, as well as delivering them inside the cells.

1.8.1. Chitosan-based formulation methods

Therefore, and as described before, the use of different formulation methodologies allows the formation of systems with very distinct characteristics. In this sense, the most widely used are ionic crosslinking, precipitation or flocculation, solvent evaporation, spray drying and chitosan coating solution, which are further characterized in the following subsections.

1.8.1.1. Ionic crosslinking

The ionic crosslinking is the most used method for the formation of nanoparticles, especially for chitosan ones. This method is based on the addition of a negative compound into the chitosan solution. In this way, it is possible that the positive charge of the chitosan can interact with the negative charge of the crosslinker, thus allowing the formation of the delivery systems [138].

The ionotropic gelation is a method based on ionic crosslinking, where the negative charge is dropwise conjugated to the chitosan solution while it is under agitation [139]. This method is characterised by being very easy to perform as well as being a relatively low-cost method compared to the others that can be explored. Nevertheless, this formulation results in systems with low stability and a highly variable size distribution, requiring an optimization of ratios between the chitosan and the crosslinker [136,139].

1.8.1.2. Precipitation or flocculation

Through this type of technique, the nanoparticles are prepared based on the addition of sodium sulphate that serves as a precipitation agent. The use of the precipitation method leads to the formation of delivery systems with a large size range, which makes them less suitable for application [139].

1.8.1.3. Solvent evaporation

The solvent evaporation technique is a method based on differences in solute volatility, whereby a surfactant in an organic phase is added to the chitosan, forming an emulsion. After addition, the emulsion is left stirring leading to evaporation of the organic phase and formation of the nanosystems. This type of system usually presents a

spherical and uniform morphology, being widely used for the formulation of nanosystems that encapsulate hydrophobic drugs [139].

1.8.1.4. Spray drying

The method of spray drying formulation involves the dissolution of chitosan and the drug to be encapsulated together, with the possibility of applying a crosslinker to ensure greater stability. Subsequently the solution are sprayed in a drying chamber causing the solvent to evaporate and the nanoparticles to form [139].

The systems formed generally have a uniform and spherical morphology as well as a fairly uniform size range [139][140]. However, the use of hot air can degrade the drug to be encapsulated, especially in the case of flavonoids which have a very poor stability.

1.8.1.5. Chitosan coating solution

This technique is based on the addition of a chitosan solution to a previously formulated chitosan nanoparticle solution [139]. In this way, nanoparticles are covered with an outer chitosan layer that allows them to have a more uniform and spherical morphology as well as a controlled release of the encapsulated drug.

Chapter 2 – Objectives

The aim of this master's thesis is to develop suitable delivery systems for quercetin encapsulation, one of the main flavonoids with a proven carcinogenic and E6 oncoprotein inhibition effect, improving its bioavailability. Therefore, some techniques have been explored to enable their encapsulation and promote their delivery to target cells.

Several types of systems made of Chitosan/TPP, Sulfobutyl-ether-β-Cyclodextrin and Chitosan/Sulfobutyl-ether-β-Cyclodextrin will be evaluated in order to select those that give rise to the best properties, namely a reduced size, an acceptable surface charge, a high encapsulation efficiency and an uniform and spherical morphology.

The systems that present the most suitable properties will then be tested in cell viability assays and calculation of half inhibitory concentration in order to understand if there is an improvement of the effect of quercetin encapsulated in these systems in relation to free quercetin.

Chapter 3 – Materials and methods

3.1. Materials

Medical grade high molecular weight (HMW) chitosan was acquired from Heppe Medical (Halle, Germany). TPP and sodium sulfobutyl ether beta-cyclodextrin (SBE-β-CD) was obtained from Acros Organics (Thermo Fisher Scientific,Waltham, MA, USA). Quercetin was kindly given by Professor Ana Paula Duarte.

HeLa cells were purchased from PromoCell (Heidelberg, Germany). DMEM/F12 cell culture media was obtained from Gibco (Thermo Fisher Scientific, Waltham, MA, USA). 3-(4,5-dimethylthiazol-2-yl)-2,5-diphenyltetrazolium bromide (MTT) was obtained from Alfa Aesar (Waltham, MA, USA).

All solutions were freshly prepared by using ultra-pure grade water, purified with a Milli-Q system from Millipore (Billerica, MA, USA).

3.2. Methods

3.2.1. Preparation of Chitosan/TPP/Quercetin nanoparticles

Stock solutions of chitosan (1 mg/mL) were prepared by resuspending the respective chitosan powder in sodium acetate buffer (0.1 M, pH 4.6) or in acetic acid 2% (pH 3.5) for 24h at 500 rpm. The chitosan used in all formulations had a HMW with a range between 200 and 500 kDa. TPP stock solutions (1 mg/mL) were prepared using the same two buffers and the same procedure. These solutions were filtered with a 450 nm filter and stored at room temperature until use.

Quercetin stock solution (300 μM) was prepared by dissolving the quercetin powder in a 50% ethanol solution for 24h at 500 rpm. The solution was stored and protected from light at 4ºC until use.

Nanoparticles were formulated using the ionotropic gelation technique. Briefly, each nanoparticle condition was formulated by adding, drop by drop, 150 μL of quercetin (300 μM) and 100 μL of TPP to 400 μL or 500 μL of chitosan. The different conditions were performed by using different concentrations and amounts of each chitosan (from

0.1 to 1 mg/mL and 400 µL or 500 µL) and different concentrations of TPP (from 0.25 to 0.75 mg/mL). The formulation of these nanoparticles was performed by exploring the positive charge of chitosan and the negative charge of TPP. The formation of these delivery systems enables the interaction with quercetin, which due to its hydrophobic behaviour, has a higher affinity to be encapsulated inside the system.

Chitosan/TPP/Quercetin nanoparticles were left for 30 minutes at room temperature for stabilization. Thereafter, these nanoparticles were centrifuged at 10.000 rpm for 10 minutes at 4ªC.

3.2.2. Preparation of SBE-β-CD/Quercetin inclusion complexes

SBE-β-CD/quercetin inclusion complex was formulated by mixing 30 mg of SBE-β-CD and 0.3 mg of quercetin powder in 5 mL of ultrapure water. The solution was left under stirring, protected from light, for 24h at 37ºC and 500 rpm. The maximum amount of quercetin that can be encapsulated within the SBE-β-CD inclusion complex had already been calculated by Nguyen and co-workers and their solubilization straight was applied to guarantee that the maximum amount of quercetin was encapsulated [106].

Before the characterization of these inclusion complexes, they were centrifuged at 12.000 rpm for 10 minutes at 4ºC.

3.2.3. Preparation of Chitosan/ SBE-β-CD/Quercetin delivery systems

Stock solution of chitosan (2 mg/mL) was prepared by resuspending HMW chitosan powder in 2% acetic acid (pH 3.5). Chitosan stock solution was filtered with a 450 nm filter and was stored at room temperature until use. SBE-β-CD/Quercetin inclusion complexes was prepared as described before.

Chitosan/SBE-β-CD/Quercetin nanoparticles were formulated by adding, drop by drop, 100 µL of different concentrations of SBE-β-CD/Quercetin (from 6mg/mL to 1.5 mg/mL of SBE-β-CD) to 300 or 400 µL of different concentrations of HMW chitosan solution (from 2 mg/mL to 1 mg/mL).

These nanoparticles were left stabilizing for 30 minutes and then were centrifuged at 10.000 rpm for 20 minutes at 4ºC.

3.2.4. Characterization of the delivery systems

Nanoparticles characterization was performed by Dynamic Light Scattering (DLS) at 25°C using a Zetasizer Nano ZS equipment (Malvern Instruments, UK) and the Malvern Zetasizer software v6.36. The evaluation of each delivery system conditions was evaluated by measure its size, PdI and zeta potential. To measure the size and PdI, all nanoparticles solution was mixed with ultra-pure water to make up 1 mL and was placed in a disposable cell. To evaluate the zeta potential, all types of nanoparticles were centrifuged as described before and were resuspended in 750 µL of ultra-pure water. All parameters were measured three times from three independent samples (n=3).

3.2.5. Determination of encapsulation efficiency

To determine the encapsulation efficiency of the best ratios of each type of delivery system, the formulations were centrifuged, as described before, and were resuspended in the same volume of methanol. Then, the samples were sonicated for 10 minutes and centrifuged for 5 minutes at 8000 rpm and 4°C as described by Sundararajan and co-workers [82]. Finally, the supernatant was recovered and the quercetin content was quantified using high-performance liquid chromatography (HPLC).

For the quercetin quantification by HPLC, 100 µL of each sample was injected in a C18 column (150 mm x 4.6 mm x 5 µm) and detected using a PDA detector at an ultraviolet wavelength of 374 nm. The analytical chromatograms were carried out using an isocratic elution system containing ultra-pure water/5% acetic acid (volume/volume (v/v))/acetonitrile (40:30:30, v/v/v) with a constant flow rate of 1 mL/min as described by Kim and co-workers [103]. Quercetin concentrations were determined through the peak areas of HPLC chromatograms for each sample. A standard curve was previously obtained with standards concentrations of quercetin dissolved in methanol. All the conditions were performed three independent assays (n=3).

3.2.6. Scanning electron microscopy

The morphology and geometry of the best ratios of each type of quercetin-loaded delivery system were evaluated using a scanning electron microscopy (SEM). Each type of delivery system was centrifuged as described before and the pellet was resuspended in 200 µL of ultra-pure water and was centrifuged as 9500 rpm during 12 minutes at

4ºC. This step was repeated three times to ensure that all the impurities were removed. After the last centrifugation, the supernatant was removed and the nanoparticles were resuspended in 40 μL of tungsten 2%. Each sample was then diluted 1:20 in ultra-pure water and 10 μL was placed in a roundly shaped coverslip. The samples were left drying at room temperature overnight.

At the next day, the samples were sputter coated with gold using an Emitech K550 (London, England) sputter coater. A SEM Hitachi S-2700 (Tokyo, Japan) was used with an acceleration of 20 kV at various magnifications to evaluate the morphology and geometry of each type of delivery system.

3.2.7. Fourier Transform Infrared Spectroscopy

To evaluate the interaction between the compounds of each type of delivery system, fourier transform infrared spectroscopy (FTIR) was performed. To prepare the samples, each type of formulation was centrifuged as described before and the pellet was resuspended in 400 μL of ultra-pure water. Each formulation was then freeze-dried at -80ºC and then lyophilized for 24h using a ScanVac Coolsafe freeze dryer (Labogene, DK).

The spectra of each isolated component and each prepared delivery system were then acquired using a Nicolet iD10 FTIR spectrophotometer (Thermo Scientific, Waltham, USA) with an average of 120 scans, a spectral resolution of 32 cm^{-1} and a spectral width ranging from 4000 and 400 cm^{-1}.

3.2.8. Cell culture

HPV18 positive cells (HeLa) were cultured in Dulbecco's Modified Eagle's Medium/Ham's F-12 nutrient mixture (DMEM-F12), supplemented with 10% (v/v) fetal bovine serum and a mixture of penicillin (100 mg/mL) and streptomycin (100 mg/mL).

Cells were grown in 25 cm^3 T-flasks at 37ºC and in a 5% CO_2 humidified atmosphere until 80% confluence be obtained.

3.2.9. Cell viability assays

Cell viability assays were performed by the MTT method, which allows to evaluate the metabolic activity of cells by the formation of formazan crystals.

Briefly, 5 x 10^3 HeLa cells were seeded in 96-well plates for 24h. Afterwards, the medium was discarded and 100 µL of fresh medium containing different concentrations of quercetin-loaded delivery systems were added to each well. Quercetin-loaded delivery systems were tested at concentrations of 10 µM, 80 µM and 150 µM. Ethanol-treated cells and free quercetin were also tested as positive controls. After 48 and 72h of incubation, medium containing delivery systems was removed and cells were washed with 100 µL of phosphate-buffered saline (PBS) to remove all the impurities. Then, MTT solution (0.5 mg/mL) was prepared by dissolving MTT powder in serum-free medium and 100 µL was added to each well, followed by incubation for 4h at 37ºC.

After the incubation period, the medium was removed and 100 µL of dimethyl sulfoxide (DMSO) was added to dissolve the formazan crystal. The redox activity was quantified through the absorbance measured at 570 nm, using the microplate reader Bio-Rad xMark spectrophotometer (Bio-Rad, EUA). Cell viability values were presented as percentages relative to the absorbance observed in non-treated cells.

IC_{50} for 48h of incubation was calculated for the quercetin-loaded delivery system that presented the best results in viability reduction assays. IC_{50} for free quercetin was also performed as comparative control.

Chapter 4 – Results and discussion

4.1. Development of Chitosan/TPP/Quercetin delivery systems

As mentioned earlier, quercetin has a well proven anti-cancer power although it has a low bioavailability. In this sense, a system based on chitosan and TPP was explored to improve the solubility and biodistribution of quercetin, considering this polymer has been widely used in the working group for the delivery of plasmid DNA [136,137]. The ionotropic gelation technique was applied for the formulation of these systems, as previously described in subsection 1.8.1.1. The stability of the systems was ensured by an ideal conjugation between the positive charges of chitosan and the negative charges of TPP [136,141].

In this sense, in order to ensure the stability of the system, characterization studies based on size and PdI measurement of the systems were performed using Zetasizer Nano ZS equipment to understand which is the best ratio of chitosan/TPP/quercetin. To optimise the ratios, the volume and concentration of quercetin (150 µL and 300 µM) and the volume of TPP (100 µL) were fixed. The volume of chitosan (500 µL or 400 µL), the concentration of chitosan (from 1 mg/mL to 0.1 mg/mL) and the concentration of TPP (0.75, 0.5 and 0.25 mg/mL) were varied. The solution, where chitosan and TPP are dissolved, was changed in order to verify if there was an improvement in the formulation of systems and the encapsulation of quercetin. An acetate buffer solution (pH 4.5) was tested first and then a 2% acetic acid solution (pH 3.5).

According to the literature, one of the factors that most influences cellular internalization is the size of the delivery systems. It is advisable that delivery systems ideally have a size less than 200 nm but can reach 500 nm depending on the type of system under study [142,143].

Another factor that also influences cellular internalization is the surface charge of the delivery systems. Positively charged nanoparticles are the most efficient at cell-membrane penetration and cellular internalization due to their effective binding to negatively charged groups on the cell surface [144]. According to the literature, a comparative study on HeLa cells of the endocytosis action with either a negative or positive superficial charged nanosystem, demonstrated that the charge significantly

affects not only their internalization ability but also the cellular endocytosis mechanism, being the positively charged nanoparticles internalized faster [145]. For this reason, it is recommended that this parameter has a value between +10 and +30 mV, so that it provides a positive charge that favours interaction with the cell membrane, without being excessively cationic to avoid toxicity and agglomeration [146]. Thus, ratios that presented a size below 500 nm, the zeta potential was further measured in order to understand if this delivery system is suitable for the cell internalization.

In the case of using chitosan and TPP dissolved in acetate buffer and for a chitosan volume of 500 µL, the size and PdI data of all the ratios tested, as well as the zeta potentials of the ratios that showed sizes smaller than 500 nm, are summarised in Table 6.

Table 6: Preparation conditions, mean size, polydispersity index and average zeta potential for chitosan/TPP/quercetin delivery system obtained with 500 µL of chitosan and 100 µL of TPP dissolved in acetate buffer. The values already present the media of three independent assays (n=3).

Chitosan concentration (mg/mL)	Chitosan volume (µL)	TPP concentration (mg/mL)	Size (nm)	PdI	Zeta potential (mV)
1	500	0.75	266.78 ± 40.75	0.423 ± 0.036	+ 21.13 ± 2.06
0.75	500	0.75	1467 ± 611.2	0.888 ± 0.129	
0.6	500	0.75	2281 ± 228.4	1	
0.5	500	0.75	848.1± 222.8	0.787 ± 0.133	
0.4	500	0.75	8628 ± 3299	0.853 ± 0.255	
0.25	500	0.75	1967 ± 214.7	1	
1	500	0.5	10527 ± 1476	0.902 ± 0.169	
0.75	500	0.5	16285 ± 8047	0.733 ± 0.231	
0.6	500	0.5	6358 ± 984.5	1	
0.5	500	0.5	1672.7 ± 272.6	1	
0.4	500	0.5	2346 ± 818.7	1	
1	500	0.25	21391 ± 14040	0.835 ± 0.144	
0.75	500	0.25	4589.7 ± 1643	1	
0.6	500	0.25	5086 ± 2007	1	
0.5	500	0.25	2512 ± 699.1	1	
0.4	500	0.25	32390 ± 14320	0.72 ± 0.245	

The analysis of results showed only the creation of nanosystems with a size less than 500 nm for the ratio of 1 mg/mL chitosan and 0.75 mg/mL TPP, where they showed a size of 266.7 nm and a PdI of 0.423. The zeta potential of this ratio was +21.13 mV, which indicated a surface charge that favours the interaction with the negative membrane of the cells, thereby facilitating its internalization. All other tested ratios showed a high size, indicating that may have occurred agglomeration of the systems. PdI values was also indicative of systems agglomeration, since they are very close to one, suggesting a high polydispersity of the samples.

The same preparation conditions were performed only changing the volume of chitosan from 500 µL to 400 µL, and the results are summarised in Table 7.

Table 7: Preparation conditions, mean size, polydispersity index and average zeta potential for chitosan/TPP/quercetin delivery system obtained with 400 µL of chitosan and 100 µL of TPP dissolved in acetate buffer. The values already present the media of three independent assays (n=3).

Chitosan concentration (mg/mL)	Chitosan volume (µL)	TPP concentration (mg/mL)	Size (nm)	PdI	Zeta potential (mV)
1	400	0.75	3963 ± 377.5	0.332 ± 0.113	
0.75	400	0.75	1447 ± 831.1	0.853 ± 0.161	
0.6	400	0.75	247.8 ± 36.3	0.359 ± 0.069	+ 40.5 ± 1.41
0.5	400	0.75	452.1 ± 39.39	0.470 ± 0.017	+ 37.2 ± 4.01
0.4	400	0.75	535.1 ± 31.05	0.53 ± 0.036	
0.25	400	0.75	2592 ± 3348	0.070 ± 0.658	
1	400	0.5	436.3 ± 80.40	0.471 ± 0.034	+ 39.5 ± 11.1
0.75	400	0.5	530.5 ± 221.3	0.553 ± 0.121	
0.5	400	0.5	319.2 ± 214.0	0.420 ± 0.210	
0.25	400	0.5	297.9 ± 131.7	0.387 ± 0.104	
1	400	0.25	1224 ± 1287	0.856 ± 0.102	
0.75	400	0.25	3819 ± 330.9	0.636 ± 0.257	
0.5	400	0.25	5380 ± 585.5	1	
0.25	400	0.25	2914 ± 1323	1	

The decrease in the volume of chitosan led to a greater proportion of quercetin in the system, thus causing different results from the data presented in Table 6. The ratio that presented the smallest size was the one containing 0.6 mg/mL of chitosan and 0.75 mg/mL of TPP. However, other ratios also presented sizes below 500 nm or very close to this value. Zeta potentials were measured for the ratios that showed the best sizes.

The ratio that showed lower size presented a surface charge (+71.92 mV) higher than the one usually recommended for cell internalization (≈ +30 mV) [146].

The use of systems dissolved in acetate buffer showed a very accelerated degradation of quercetin through the time, thus making the application of this strategy not suitable for the formulation of quercetin delivery systems. Thus, and taking into consideration the literature, it was possible to verify that the use of 2% acetic acid at a pH of 3.5 allowed the solubilization of chitosan and TPP as well as a high stability of quercetin [42,103]. In this way, the same procedure that was carried out for the delivery systems components dissolved in acetate buffer, was also performed for the acetic acid solution.

For the 500 µL volume of chitosan in 2% acetic acid, ratios of chitosan between 1 and 0.1 mg/mL and TPP between 0.75 and 0.25 mg/mL were tested. The summary of the obtained results of size and surface charge of systems with smaller sizes are shown in Table 8.

Table 8: Preparation conditions, mean size, polydispersity index and average zeta potential for chitosan/TPP/quercetin delivery system obtained with 500 µL of chitosan and 100 µL of TPP dissolved in acetic acid 2%. The values already present the media of three independent assays (n=3).

Chitosan concentration (mg/mL)	Chitosan volume (µL)	TPP concentration (mg/mL)	Size (nm)	PdI	Zeta potential (mV)
1	500	0.75	245.5 ± 31.50	0.408 ± 0.083	+ 79.63 ± 3.16
0.75	500	0.75	1924.5 ± 371.67	1	
0.6	500	0.75	2545 ± 1127.8	1	
0.5	500	0.75	2606 ± 1617	1	
0.4	500	0.75	325.1 ± 193.2	0.371 ± 0.197	+ 16.6 ± 1.08
0.25	500	0.75	3183.25 ± 62.93	0.564 ± 0.005	
0.1	500	0.75	2690 ± 715.6	0.403 ± 0.207	
1	500	0.5	504.1 ± 193.4	0.483 ± 0.113	+ 85.0 ± 18.1
0.75	500	0.5	990.17 ± 180.93	0.634 ± 0.081	
0.6	500	0.5	7002 ± 1028.84	0.394 ± 0.054	
0.5	500	0.5	18774 ± 1224	0.202 ± 0.142	
0.4	500	0.5	1460 ± 48.08	0.809 ± 0.029	
0.25	500	0.5	408.75 ± 193.1	0.486 ± 0.122	+ 50.57 ± 6.03
0.1	500	0.5	2239 ± 236.17	0.369 ± 0.030	
1	500	0.25	1063.29 ±328.1	0.589 ± 0.200	
0.75	500	0.25	1626 ± 403.05	0.657 ± 0.199	

0.6	500	0.25	4380 ± 254.56	0.363 ± 0.408
0.5	500	0.25	3061 ± 91.21	0.802 ± 0.141
0.4	500	0.25	3142 ± 523.2	0.832 ± 0.243
0.25	500	0.25	4020 ± 1079.8	0.940 ± 0.074
0.1	500	0.25	2854 ± 1023.4	0.036 ± 0.028

The use of acetic acid in the preparation of a chitosan solution of 1 mg/mL and TPP solution of 0.75 mg/mL showed a reduced size of 245.5 nm and a PdI of 0.408 when a volume of chitosan of 500 µL was used in the formulations. Nonetheless, the surface charge measurement of the systems indicated +79.63 mV, which can be too high for subsequent cell internalization causing toxicity due to the excess of cationic charges.

On the other hand, for a chitosan concentration of 0.4 mg/mL and TPP concentration of 0.75 mg/mL it was obtained a size of 325.1 nm, a PdI of 0.371 and a zeta potential of +16.6 mV. Therefore, this ratio although presenting a slightly bigger size, shows a zeta potential suitable for cell internalization, making this ratio the most indicated to be consider for the formation of delivery systems for *in vitro* assays.

The volume reduction of chitosan to 400 µL was also performed in the case of the solutions diluted in acetic acid, and the summary of the obtained average sizes is presented in Table 9.

Table 9: Preparation conditions, mean size, polydispersity index and average zeta potential for chitosan/TPP/quercetin delivery system obtained with 400 µL of chitosan and 100 µL of TPP dissolved in acetic acid 2%. The values already present the media of three independent assays (n=3).

Chitosan concentration (mg/mL)	**Chitosan volume (µL)**	**TPP concentration (mg/mL)**	**Size (nm)**	**PdI**
1	400	0.75	6021 ± 1043.1	1
0.75	400	0.75	1880 ± 1591.0	0.8 ± 0.707
0.5	400	0.75	1471 ± 645.32	1
0.25	400	0.75	4130 ± 2014.2	0.315 ± 0.12
1	400	0.5	2272 ± 1740.2	1
0.75	400	0.5	3871 ± 609.53	0.584 ± 0.294
0.5	400	0.5	2358 ± 1069.9	0.87 ± 0.092
0.25	400	0.5	2028 ± 2649.5	0.769 ± 0.163
1	400	0.25	2212 ± 523.97	0.737 ± 0.186
0.75	400	0.25	6918 ± 615.18	1

0.5	400	0.25	2856 ± 960.25	1
0.25	400	0.25	3218 ± 704.28	1

The results presented in Table 9 showed that the reduction of chitosan volume to 400 µL led to non-formation or agglomeration of the systems, independent of the chitosan/TPP ratio used. Considering that no ratio gave values below 500 nm, no zeta potential was measured.

Decreasing the concentration of TPP to 0.25 mg/mL led to non-formation of systems due to the low number of negative charges in the system to crosslink the positive charges of chitosan polymer. This observation is applied for both the 500 µL and 400 µL volume of chitosan.

In summary, with the experiments of chitosan and TPP dissolved in acetate buffer and acetic acid, it was possible to visualize ratios where the delivery system could be suitable for delivery into cells and subsequent cellular internalization. However, and as previously mentioned, the delivery systems with chitosan and TPP dissolved in acetic acid allowed a high stability of the encapsulated drug. In this manner, the formulations having both chitosan and TPP dissolved in acetic acid were selected to proceed to further studies, with the best ratio being defined considering the size, PdI and surface charge presented. Thus, the delivery systems formulated with 500 uL of 0.4 mg/mL chitosan and a TPP concentration of 0.75 mg/mL, were selected since they showed a size of 325.1 nm, a PdI of 0.371 and a surface charge of +16.6 mV.

4.2. Development of SBE-β-CD delivery systems

As previously mentioned, the use of inclusion complexes such as SBE-β-CD can be a potential strategy for the encapsulation of hydrophobic drugs, such as quercetin, thus facilitating their delivery into cells as well as its stability and bioavailability.

In order to check whether the size of formulations is influenced by the concentration of cyclodextrins, several concentrations of SBE-β-CD were tested and the values of the average sizes as well as the surface charge of the best ratio are summarised in Table 10.

Table 10: Average size, PdI and zeta potential of SBE-β-CD based delivery systems with quercetin for the various ratios. The values already present the media of three independent assays (n=3).

SBE-β-CD concentration (mg/mL)	Size (nm)	PdI	Zeta potential (mV)
6	2782.5 ± 974.6	1	
3	2468.33 ± 207.4	0.123 ± 0.019	- 21.03 ± 0.723
1.5	1758 ± 410.6	1	

The size values presented in Table 9 indicate a high agglomeration of the cyclodextrins. This factor may be due to an excess of negative charges in the system, since the cyclodextrin chosen presents a negative charge, and also to the fact that it has sodium in its constitution in order to stabilise the negative charges and its presence can create some agglomerates [125,147]. Thus, regardless of the ratio chosen, the systems always presented sizes higher than 500 nm, which could limit their internalization process in cells. Since the SBE-β-CD concentrations of 6 mg/mL and 1.5 mg/mL systems presented a PdI of 1, it was understandable that the system sizes showed a high range of values and therefore were not suitable to be used in further studies. For the cyclodextrin concentration of 3 mg/mL, although the size was still larger than desired, the PdI presented was only 0.123, monodispersity being for that reason the most suitable system to be used in *in vitro* studies. The surface charge was measured for this ratio and a value of -21.03 mV was obtained, thus indicating surface charge as one more limiting factor of cell internalization caused by the repulsion of anionic charges [146].

4.3. Development of Chitosan/SBE-β-CD delivery systems

Since the systems containing only SBE-β-CD and quercetin obtained a very high size compared to what it is expected, a conjugation of these systems with chitosan was made, through the ionotropic gelation technique, as indicated previously.

Optimization of chitosan/SBE-β-CD/quercetin systems was performed by keeping constant the volume of the SBE-β-CD/quercetin solution (100 µL) and changing its concentration (between 6 mg/mL and 1.5 mg/mL), chitosan concentration (between 2 and 1 mg/mL) and chitosan volume (400 µL or 300 µL). For a chitosan volume of 400 µL, the respective average sizes and PdI are summarised in Table 11.

Table 11: Average size and PdI of delivery systems based on chitosan and SBE-β-CD with quercetin for the various ratios and for a chitosan volume of 400 µL. The values already present the media of three independent assays (n=3).

Chitosan concentration (mg/mL)	Chitosan volume (µL)	SBE-β-CD concentration (mg/mL)	Size (nm)	PdI
2	400	6	964.07 ± 22.32	0.562 ± 0.118
1.5	400	6	318.6 ± 2.18	0.271 ± 0.009
1	400	6	303.63 ± 1.89	0.25 ± 0.007
2	400	4.5	3129 ± 756.44	1
1.5	400	4.5	2399 ± 47.38	1
1	400	4.5	329.3 ± 3.78	0.309 ± 0.007
2	400	3	2654 ± 627.94	1
1.5	400	3	3256.67 ± 761.05	1
1	400	3	485.73 ± 9.30	0.336 ± 0.019
2	400	1.5	3320 ± 896.61	0.801 ± 0.141
1.5	400	1.5	2890 ± 304.06	1
1	400	1.5	1662 ± 40.36	0.093 ± 0.004

Taking into consideration the data present in Table 11, it was possible to verify a lower size of 303.63 nm and a PdI of 0.25 for the systems with a chitosan concentration of 1 mg/mL and a SBE-β-CD concentration of 6 mg/mL. However, better results were obtained by performing the same procedure and only change the chitosan volume from 400 µL to 300 µL, with the size, PdI and zeta potential values summarized in Table 12.

Table 12: Average size and PdI of delivery systems based on chitosan and SBE-β-CD with quercetin for the various ratios and for a chitosan volume of 300 µL. For the best ratios, superficial charge measurements were also realized. The values already present the media of three independent assays (n=3).

Chitosan concentration (mg/mL)	Chitosan volume (µL)	SBE-β-CD concentration (mg/mL)	Size (nm)	PdI	Zeta potential (mV)
2	300	6	404.5 ± 4.68	0.314 ± 0.009	
2	300	4.5	4330 ± 557.20	1	
1.5	300	4.5	433.03 ± 16.43	0.424 ± 0.074	
1	300	4.5	289.07 ± 2.02	0.261 ± 0.013	+34.27 ± 0.55
2	300	3	2714.67 ± 927.87	1	
1.5	300	3	1379.5 ± 164.76	1	
1	300	3	272.07 ± 2.87	0.287 ± 0.011	+ 38 ± 1.34
2	300	1.5	3104 ± 438.73	0.592 ± 0.204	

1.5	300	1.5	2960 ± 1252.61	0.826 ± 0.239
1	300	1.5	1151.23 ± 536.35	0.934 ± 0.069

According to Table 11, better results were obtained by decreasing the chitosan volume from 400 µL to 300 µL, and a size of 272.07 nm and a PdI of 0.287 were obtained for a concentration of 1 mg/mL chitosan and 3 mg/mL SBE-β-CD. Within the Chitosan/SBE-β-CD/Quercetin systems, this was the ratio that presented the best characteristics. The surface charge was subsequently measured, being obtained +38.0 mV, a value only slightly above what is desirable for cell internalization.

4.4. Encapsulation efficiency

The encapsulation efficiency of quercetin depends on several factors, being the affinity between the hydrophobicity of the drug and the hydrophobic domains of the delivery system one of the most relevant [64]. On the other hand, and taking into consideration that quercetin has almost null aqueous solubility, the use of aqueous solutions in the systems leads to quercetin molecules being forced to interact with the delivery systems formed and, thus, increasing its encapsulation [64]. In this aspect and taking into consideration that in the formulation of chitosan/TPP/Quercetin delivery systems, quercetin is dissolved in a 50% ethanol solution, the interaction of quercetin with the system may be less than desirable, thus reducing its encapsulation.

Thus, in order to understand the amount of quercetin encapsulated in each type of delivery system, the encapsulation efficiency was measured using HPLC. The results obtained are presented in Table 13.

Table 13: Encapsulation efficiency, in percentage, for the optimized ratio of each type of delivery system. The data were obtained through the average of triplicates (n=3).

Delivery system	**Encapsulation efficiency (%)**
Chitosan/TPP/Quercetin	10.80
SBE-β-CD/Quercetin	≈ 100
Chitosan/SBE-β-CD/Quercetin	≈ 100

The results present in Table 12 showed low quercetin encapsulation for the chitosan/TPP systems, indicative that these systems have a low number of hydrophobic domains where quercetin can bind. On the other hand, systems that have cyclodextrins, a compound that has a hydrophobic cavity, showed an almost total encapsulation rate, this being due to the high number of hydrophobic domains present in the system where quercetin can bind. In addition, the quercetin concentration was optimised following the work of Nguyen and co-workers as described above, which allowed to place the maximum concentration of quercetin that could be encapsulated in the optimized chitosan/SBE-β-CD conditions [106].

Thus, systems composed by SBE-β-CD allow a higher ratio between quercetin and the system, thus making these formulations more efficient for payload encapsulation.

4.5. Scanning electron microscopy

The morphology of the delivery systems can also influence cellular internalization, so it is of high relevance to verify if the delivery systems have a regular and spherical morphology. In this way, and using SEM, images were captured for each type of formulated system, and are presented in Figure 16.

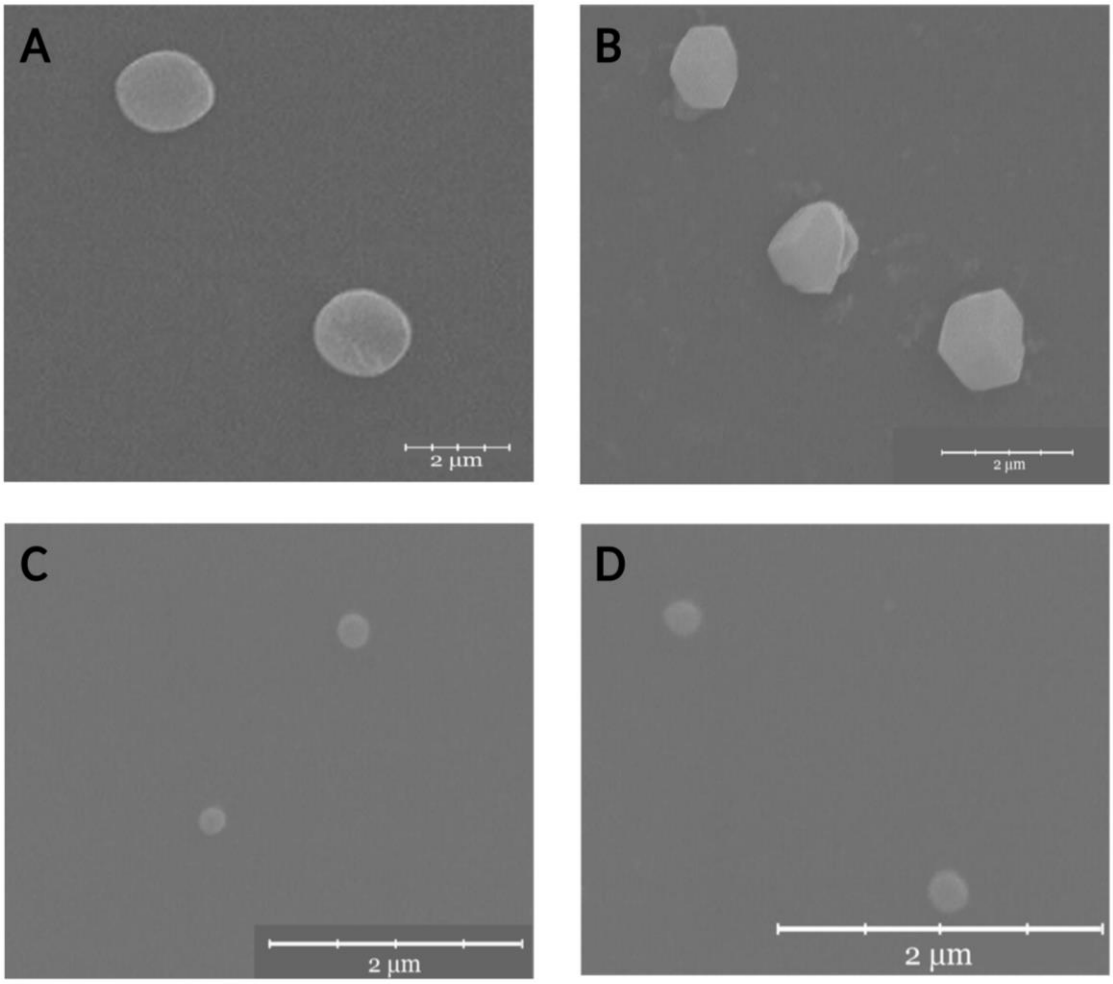

Figure 16: Delivery systems images obtained by SEM. (A) Chitosan/TPP/Quercetin delivery systems; (B) SBE-β-CD/Quercetin delivery systems; (C) and (D) Chitosan/SBE-β-CD/Quercetin delivery systems.

For chitosan-based systems, an uniform and spherical morphology was observed, what can favour their cellular internalization. However, for the SBE-β-CD and quercetin delivery systems it was possible to verify a non-uniform and non-rounded morphology, also presenting many agglomerates, thus making their application in cells limited.

4.6. UV/Vis absorbance spectrum

In order to understand the interactions that arise with the formulation of systems, the UV-vis absorption spectra were plotted for each component of each type of system and are presented in Figure 17.

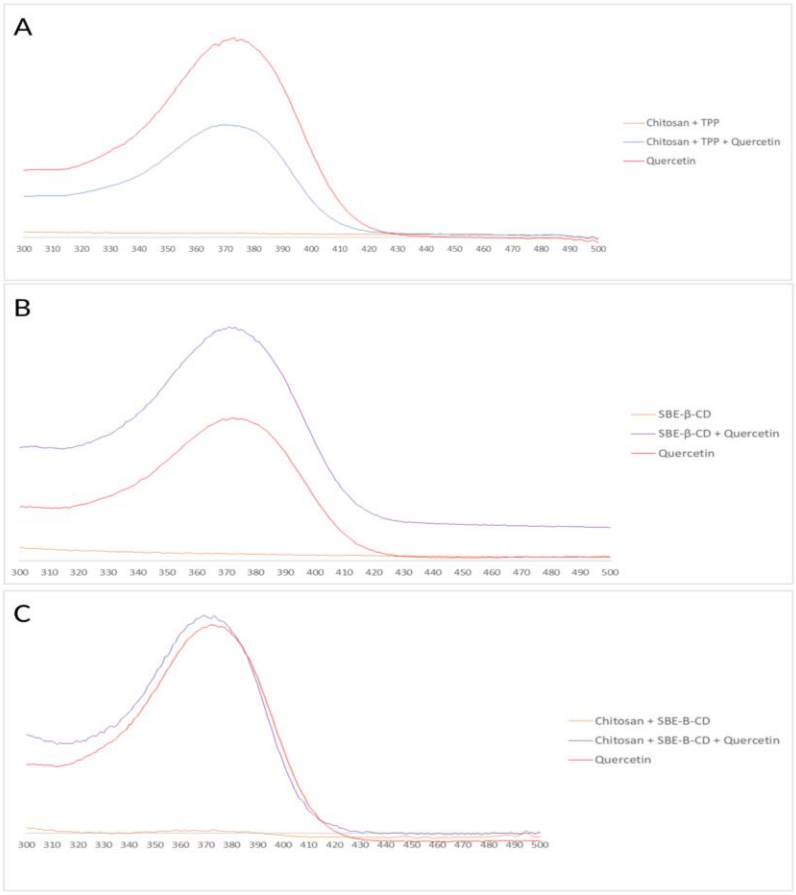

Figure 17: UV-vis spectra for each component and for the formulated delivery systems of (A) Chitosan/TPP/Quercetin; (B) SBE-β-CD/Quercetin; (C) Chitosan/SBE-β-CD/Quercetin.

For the chitosan/TPP/quercetin delivery systems shown in Figure 17.A, it was verified that quercetin exhibits a significant peak near 374 nm while the chitosan/TPP spectrum does not show any significant peak. In the case of complete systems with chitosan, TPP and quercetin, it was obtained a significant peak around 374 nm with a lower absorbance than the one observed in free quercetin spectrum, indicating an interaction with the drug.

In the case of SBE-β-CD/Quercetin delivery systems, the same study was carried out being presented in figure 17.B. Here, it was observed that SBE-β-CD did not show a significant peak but, after conjugation with quercetin, it showed a higher peak than that observed in free quercetin spectrum at the wavelength of 374 nm. Finally for the Chitosan/SBE-β-CD/Quercetin delivery systems presented in Figure 17.C, the spectrum showed a significant peak at 374 nm with an absorbance similar to that of free quercetin.

Thus, these experiments showed the interaction of quercetin with all the systems tested.

4.7. Fourier Transform Infrared Spectroscopy

To further ensure that all compounds are present in each type of delivery system, a FTIR analysis of each system was also performed. For Chitosan/TPP/Quercetin systems, the presence of specific chemical groups of each compound was evaluated as well as the interaction between each compound in the system, and the respective spectra are shown in Figure 18.

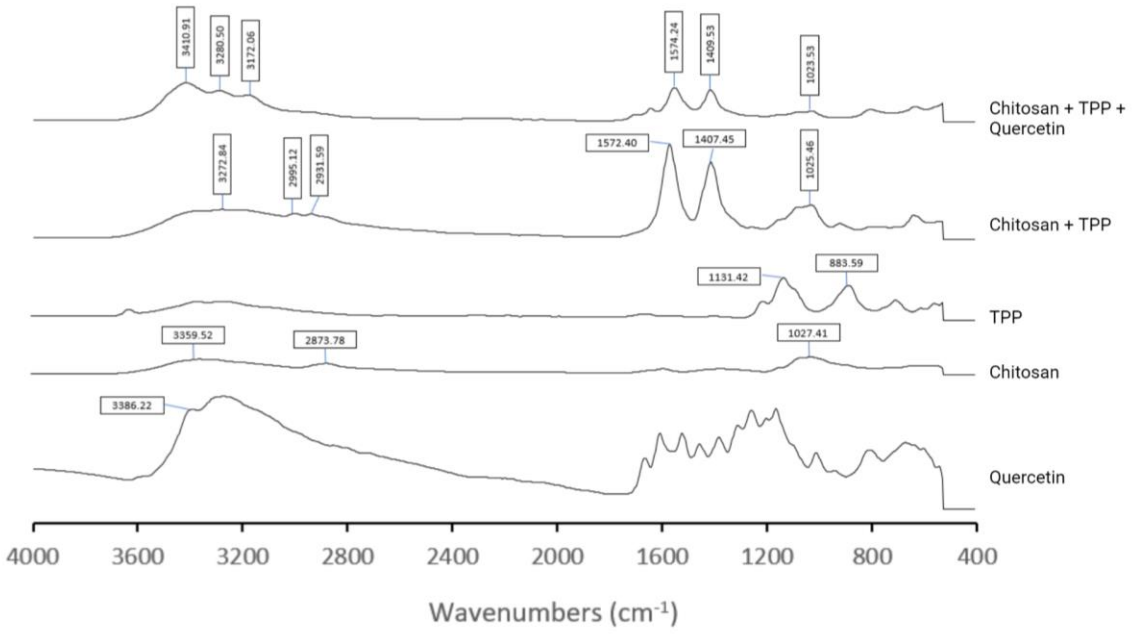

Figure 18: FTIR spectra (absorbance versus wavenumbers) of quercetin, chitosan, TPP, chitosan/TPP and chitosan/TPP/quercetin delivery systems.

Considering the spectrum of Figure 18, quercetin presents a characteristic peak at a wavelength of 3386.22 cm^{-1} attributed to the phenolic stretching vibrations of the *-OH* bonds. Additionally, it presents several peaks in the regions between 1600 cm^{-1} and 1100 cm^{-1}, corresponding to *-CO* stretching, aromatic stretching and bending and -OH phenolic bending [148]. For the case of the pure chitosan spectrum, characteristic absorption peaks were identified at the wavelength of 3359.52 cm^{-1}, corresponding to the intermolecular and intramolecular hydrogen bonds *-OH* and *-NH*; at 2873.78 cm^{-1}, corresponding to *-CH* stretching vibrations; and at 1027.41 cm^{-1}, attributed to the asymmetric stretching of the *C-O-C* bridge [64,136,149]. Similarly, the spectrum of

pure TPP showed two characteristic peaks at 1131.42 cm^{-1} and 883.59 cm^{-1}, corresponding to the *-PO* stretching vibration and to asymmetric stretching of the *P-O-P* bridge, respectively [136].

After chitosan/TPP conjugation, it was obtained a shift of the characteristic peak of chitosan from the wavelength of 3359.52 cm^{-1} to 3272.84 cm^{-1}, showing an interaction between the two compounds resulting from the alteration of the *-OH* and *-NH* bonds present in chitosan. In addition, significant peaks appeared at wavelengths of 1572.40 and 1407.45 cm^{-1} corresponding to vibrations of the *N-O-P* bonds that were formed [136]. Regarding this FTIR spectra, it was possible to evidence that TPP anions were crosslinked with the amine groups of chitosan, forming the complexes, and similar results were obtained in other works [136,150,151]. Finally, for the case of chitosan/TPP/Quercetin systems it was possible to identify a characteristic peak of quercetin, at a wavelength of 3401.91 cm^{-1}, as well as all the peaks referring to the interactions between chitosan and TPP, showing the presence and binding of all the compounds.

The same assessment was performed for the SBE-β-CD/Quercetin based systems and are shown in Figure 19.

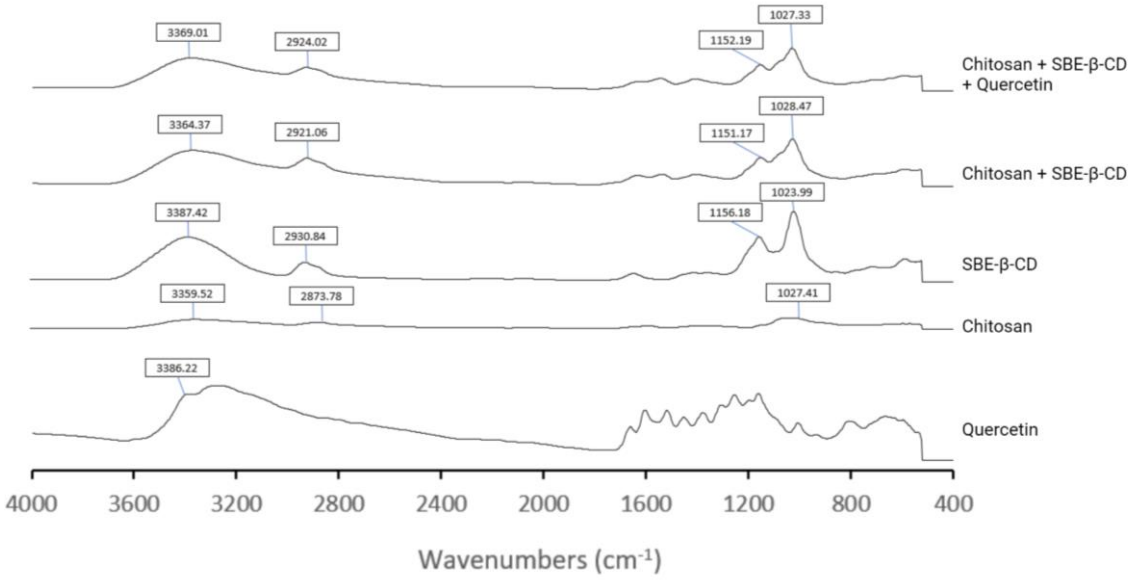

Figure 19: FTIR spectra (absorbance versus wavenumbers) of quercetin, chitosan, SBE-β-CD, chitosan/SBE-β-CD and chitosan/SBE-β-CD/quercetin delivery systems.

Taking into consideration the spectra presented in Figure 19, characteristic absorbance peaks of SBE-β-CD at the wavelength of 3387.42 cm^{-1} are observed, corresponding to

the *-OH* bonds, and at the wavelengths of 1156.18 cm-1 and 1023.99 cm-1 corresponding to the -CH bonds and the asymmetric stretching of the *C-O-C* bridge [106]. After the addition of chitosan to the SBE-β-CD complexes, characteristic peaks of each compound were obtained, with only slight changes in the wavelengths of each peak arising from the interactions formed between the compounds.

In the case of chitosan/SBE-β-CD/quercetin delivery systems, a similar spectrum to the result without quercetin was verified, due to the nature of the encapsulation system. Cyclodextrins are inclusion complexes that allow hydrophobic drugs to be "trapped", making the drug completely coated and limiting its detection by techniques such as FTIR [106]. Accordingly, the FTIR spectrum of the chitosan/SBE-β-CD/quercetin system allowed to prove that quercetin was encapsulated inside the systems and not bound to their surface. This fact is also evidenced in other similar studies [106,141,152].

4.8. Cell viability assays

In order to understand the therapeutic efficiency of quercetin delivery systems to cancer cells, an initial screening was performed for each type of system during 48h and 72h of incubation. The results of the cell viability reduction for each type of system and for free quercetin are shown in Figure 20.

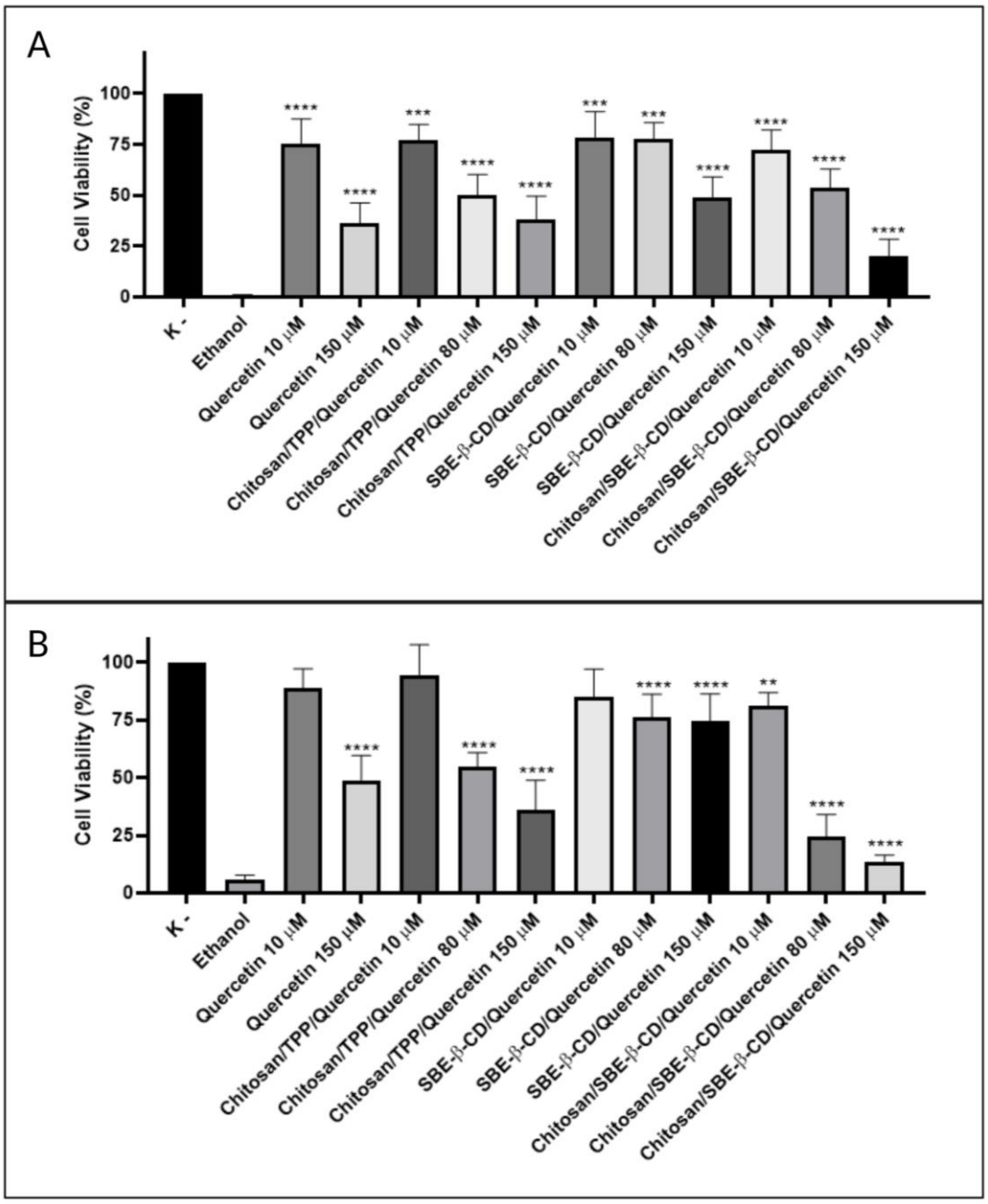

Figure 20: Cell viability assay on HeLa cells for each type of delivery system for a period of incubation of (A) 48h; (B) 72h. Non-transfected cells were used as negative control (K-) and cells treated with 70% ethanol were used as positive control. Free quercetin was used as a comparative control. Data are presented as mean ± SD for three independent experiments (n=3) and was analyzed by one-way ANOVA with the Bonferroni test. Significance was determined as ρ-values *<0.05, **<0.01, ***<0.001, ****<0.0001.

The results presented in figure 20, show that delivery systems of chitosan/TPP/quercetin and SBE-β-CD/quercetin did not induce a greater reduction in cell viability than the result presented by free quercetin. Thus, the delivery of quercetin

with these systems does not significantly increase the reduction of the viability of HPV positive cancer cells.

As for the chitosan/SBE-β-CD/quercetin systems, it was observed a higher reduction of cell viability in relation to free quercetin for both 48 and 72h of incubation, being more evident for higher concentrations of quercetin. For this type of system, a significant decrease in HPV positive cancer cells was obtained to 20.12% and 13.64% after an incubation period of 48h and 72h, respectively, for a quercetin concentration of 150 μM.

4.9. Half inhibitory concentration

Thus, having in mind the results presented in the initial screening of the viability assays, it is evident that the chitosan/SBE-β-CD/quercetin systems presented the most promising results, having for this reason been selected for the IC_{50} calculation. The incubation period selected was 48h. The same calculation was performed for free quercetin in order to serve as a positive control and allow comparison of results between the delivery of quercetin in encapsulated and free form. The results are shown in figure 21.

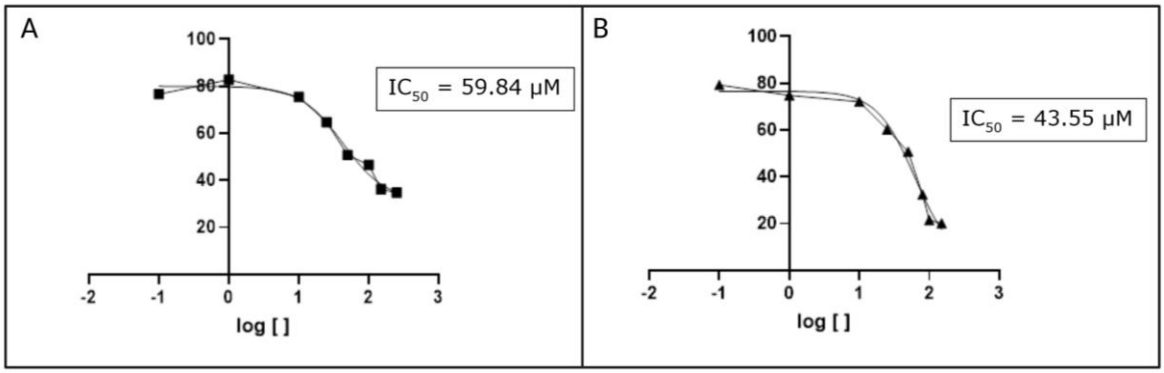

Figure 21: IC_{50} on HeLa cells for an incubation period of 48h for (A) free quercetin; (B) chitosan/SBE-β-CD/quercetin delivery systems. Data was obtained from three independent assays (n=3).

Considering the results obtained, it was possible to verify a decrease in IC_{50} from 59.84 μM to 43.55 μM with the encapsulation of quercetin in this type of delivery system, thus indicating that the use of delivery systems increases the quercetin bioavailability, and they are more effective than the application of free quercetin.

Comparing the results obtained with other quercetin delivery systems, summarised in table 5, it can be seen that there is an improvement in the therapeutic effect compared with nanoemulsions, micelles and the vast majority of synthetic polymeric systems [63,72,76,78–80]. In addition, it also showed similar results to those found in liposome-based delivery systems as well as systems formed by chitosan and quinoline, indicating an IC50 between 40 and 50 μM [58,60,64,70]. Lower IC50 values have been achieved for PEG-based delivery systems, which can reach up to 3.033 μM [59,61,71]. Nevertheless, PEG has a well-proven cell toxicity limiting its use for *in vivo* assays.

In this way, the systems formed present very promising results, and since they only consist of non-toxic compounds, enable their implementation for *in vivo* trials.

Chapter 5 – Conclusions and future perspectives

Cervical cancer has decreased in incidence and mortality but has remained a leading cause of death in less developed countries, where anti-HPV preventive vaccines are not widely administered and health care is weaker. In this sense, therapies that allow the treatment of HPV infections and cervical cancer have been studied. Flavonoids have emerged as compounds with proven anti-cancer power and quercetin has been the most clinically relevant flavonoid. Quercetin, in addition to its numerous anti-cancer properties, also has the ability to inhibit the E6 oncoprotein, which leads to an increase in p53 levels and post-induction of apoptosis. However, the vast majority of flavonoids, and especially quercetin, have a very low bioavailability, resulting from their low aqueous solubility, and easy degradation. Thus, it is important to study ways to encapsulate this type of drug and ensure its delivery to cancer cells.

The aim of this work was the development of quercetin loaded delivery systems to be applied in HPV positive cells, in order to increase the effect of quercetin. In this sense, three types of delivery systems were developed and characterized, being them made of chitosan/TPP/quercetin, SBE-β-CD/quercetin and chitosan/SBE-β-CD/quercetin. The ratios of each delivery system have been optimized in order to obtain the best sizes, PdI and surface charge of formulations. Thus, it was possible to obtain optimised delivery systems of chitosan/TPP/quercetin with a size of 325.1 nm, a PdI of 0.371 and a surface charge of +16.6 mV, delivery systems of SBE-β-CD/quercetin with a size of 2468.33 nm, a PdI of 0.123 and a surface charge of -21.03 mV and chitosan/SBE-β-CD/quercetin delivery systems with a size of 272.07 nm, a PdI of 0.287 and a surface charge of +38 mV. The encapsulation efficiency of quercetin delivery systems also differed between each type of system, with the chitosan/TPP/quercetin systems showing only a 10% encapsulation, limiting their use, compared to the other types of systems tested which showed close to 100% encapsulation.

Furthermore, all the systems were also characterised in their morphology and in interactions between their constituents, and in the case of the chitosan/TPP/quercetin delivery systems it was verified the presence of quercetin in the FTIR spectrum, indicating the presence of quercetin on the surface, while in the systems containing SBE-β-CD the same was not observed, due to the fact that it is completely encapsulated inside the inclusion complex.

Cellular viability assays also allowed to verify that chitosan/SBE-β-CD/quercetin systems showed the greatest reduction in viability among the three types of systems being tested in an initial comparative screening, with a viability of 20.13% being obtained after 48h of incubation for this type of system containing 150 μM quercetin. Subsequently these systems showed a lower IC_{50} than free quercetin, being respectively 43.55 and 59.84 μM, indicating an improved reduction of the HPV positive cancer cells viability.

Taking into consideration the results presented in this master's thesis, it was possible to observe that the encapsulation of quercetin allowed the improvement of therapeutic effect against HPV positive cells. However, as future perspectives, other studies may still be carried out, such as the quantification of p53 oncoprotein through western blot, in order to ensure that the delivery systems present an increase in the expression levels of p53, thus indicating an inhibition of the carcinogenesis processes and induction of apoptosis. Modifications to the delivery systems can also be made in order to direct them to the target cells, for example, by the addition of ligands thus enabling a greater therapeutic effect.

Chapter 6 – References

1. World Health Organization (WHO). GLOBOCAN 2020—The Global Cancer Observatory: Cancer Today—All Cancers; World Health Organization (WHO) International Agency for Research on Cancer: Lion, France, 2020. Available online: https://gco.iarc.fr/today/data/factsheets/cancers/39-All-cancers-fact-sheet.pdf (accessed on 16 December 2021).
2. Szymonowicz, K.A.; Chen, J. Biological and Clinical Aspects of HPV-Related Cancers. *Cancer Biol. Med.* **2020**, *17*, 864–878, doi:10.20892/j.issn.2095-3941.2020.0370.
3. World Health Organization (WHO). GLOBOCAN 2020—The Global Observatory: Cancer Today—Cervix Uteri; World Health Organization (WHO) International Agency for Research on Cancer: Lion, France, 2020. Available online: https://gco.iarc.fr/today/data/factsheets/cancers/23-Cervix-uteri-fact-sheet.pdf (accessed on 16 December 2021).
4. Almeida, A.M.; Queiroz, J.A.; Sousa, F.; Sousa, Â. Cervical Cancer and HPV Infection: Ongoing Therapeutic Research to Counteract the Action of E6 and E7 Oncoproteins. *Drug Discov. Today* **2019**, *24*, 2044–2057, doi:10.1016/j.drudis.2019.07.011.
5. World Health Organization (WHO). GLOBOCAN 2020—The Global Cancer Observatory—Cancer Today Low Income; World Health Organization (WHO) International Agency for Research on Cancer: Lion, France, 2020. Available online: https://gco.iarc.fr/ today/data/factsheets/populations/989-low-income-fact-sheets.pdf (accessed on 20 December 2021).
6. Stewart, B.W.; Kleihues, P. New_Drug.Pdf 2003, 181–188.
7. Doorbar, J. The Papillomavirus Life Cycle. *J. Clin. Virol.* **2005**, *32*, 7, doi:10.1016/j.jcv.2004.12.006.
8. De Villiers, E.M.; Fauquet, C.; Broker, T.R.; Bernard, H.U.; Zur Hausen, H. Classification of Papillomaviruses. *Virology* **2004**, *324*, 17–27, doi:10.1016/j.virol.2004.03.033.
9. Jung, H.S.; Rajasekaran, N.; Ju, W.; Shin, Y.K. Human Papillomavirus: Current and Future RNAi Therapeutic Strategies for Cervical Cancer. *J. Clin. Med.* **2015**, *4*, 1126–1155, doi:10.3390/jcm4051126.
10. Arbyn, M.; Castellsagué, X.; de sanjosé, S.; Bruni, L.; Saraiya, M.; Bray, F.; Ferlay, J. Worldwide Burden of Cervical Cancer in 2008. *Ann. Oncol.* **2011**, *22*, 2675–2686, doi:10.1093/annonc/mdr015.
11. Sak, K. Characteristic Features of Cytotoxic Activity of Flavonoids on Human Cervical Cancer Cells. *Asian Pacific J. Cancer Prev.* **2014**, *15*, 8007–8019, doi:10.7314/APJCP.2014.15.19.8007.

12. Lee, S.J.; Yang, A.; Wu, T.; Hung, C.F. Immunotherapy for Human Papillomavirus-Associated Disease and Cervica Cancer: Review of clinical and translational research. *J. Gynecol. Oncol.* **2016**, *27*, 1–17.

13. K. Saxena, S.; Kumar, S.; Mati Goel, M.; Kaur, A.; LB Bhatt, M. Recent Advances in Human Papillomavirus Infection and Management. *Curr. Perspect. Hum. Papillomavirus* **2019**, 1–13, doi:10.5772/intechopen.81970.

14. Choi, Y.J.; Park, J.S. Clinical Significance of Human Papillomavirus Genotyping. *J. Gynecol. Oncol.* **2016**, *27*, 1–12, doi:10.3802/jgo.2016.27.e21.

15. de Sanjosé, S.; Brotons, M.; Pavón, M.A. The Natural History of Human Papillomavirus Infection. *Best Pract. Res. Clin. Obstet. Gynaecol.* **2018**, *47*, 2–13, doi:10.1016/j.bpobgyn.2017.08.015.

16. Ferreira, M.; Costa, D.; Sousa, Â. Flavonoids-Based Delivery Systems towards Cancer Therapies. *Bioengineering* **2022**, *9*, doi:10.3390/bioengineering9050197.

17. Thomas, M.; David, P.; Banks, L. The Role of the E6-P53 Interaction in the Molecular Pathogenesis of HPV. *Oncogene* **1999**, *18*, 7690–7700, doi:10.1038/sj.onc.1202953.

18. Franconi, R.; Massa, S.; Paolini, F.; Vici, P.; Venuti, A. Plant-Derived Natural Compounds in Genetic Vaccination and Therapy for HPV-Associated Cancers. *Cancers (Basel).* **2020**, *12*, 1–38, doi:10.3390/cancers12113101.

19. Tomaić, V. Functional Roles of E6 and E7 Oncoproteins in HPV-Induced Malignancies at Diverse Anatomical Sites. *Cancers (Basel).* **2016**, *8*, doi:10.3390/cancers8100095.

20. Hoppe-Seyler, K.; Bossler, F.; Braun, J.A.; Herrmann, A.L.; Hoppe-Seyler, F. The HPV E6/E7 Oncogenes: Key Factors for Viral Carcinogenesis and Therapeutic Targets. *Trends Microbiol.* **2018**, *26*, 158–168, doi:10.1016/j.tim.2017.07.007.

21. Gomes, D.; Yaduvanshi, S.; Silvestre, S.; Duarte, A.P.; Santos, A.O.; Soares, C.P.; Kumar, V.; Passarinha, L.; Sousa, Â. Taxifolin and Lucidin as Potential E6 Protein Inhibitors: P53 Function Re-Establishment and Apoptosis Induction in Cervical Cancer Cells. *Cancers (Basel).* **2022**, *14*, doi:10.3390/cancers14122834.

22. Abotaleb, M.; Samuel, S.M.; Varghese, E.; Varghese, S.; Kubatka, P.; Liskova, A.; Büsselberg, D. Flavonoids in Cancer and Apoptosis. *Cancers (Basel).* **2019**, *11*, doi:10.3390/cancers11010028.

23. Yousefi, M.; Shadnoush, M.; Sohrabvandi, S.; Khorshidian, N.; Mortazavian, A.M. Encapsulation Systems for Delivery of Flavonoids: A Review. *Biointerface Res. Appl. Chem.* **2021**, *11*, 13934–13951, doi:10.33263/BRIAC116.1393413951.

24. Lesjak, M.; Beara, I.; Simin, N.; Pintać, D.; Majkić, T.; Bekvalac, K.; Orčić, D.; Mimica-Dukić, N. Antioxidant and Anti-Inflammatory Activities of Quercetin and Its Derivatives. *J. Funct. Foods* **2018**, *40*, 68–75, doi:10.1016/j.jff.2017.10.047.

25. Aziz, N.; Kim, M.Y.; Cho, J.Y. Anti-Inflammatory Effects of Luteolin: A Review of in

Vitro, in Vivo, and in Silico Studies. *J. Ethnopharmacol.* **2018**, *225*, 342–358, doi:10.1016/j.jep.2018.05.019.

26. Orhan, D.D.; Özçelik, B.; Özgen, S.; Ergun, F. Antibacterial, Antifungal, and Antiviral Activities of Some Flavonoids. *Microbiol. Res.* **2010**, *165*, 496–504, doi:10.1016/j.micres.2009.09.002.

27. Madunić, J.; Madunić, I.V.; Gajski, G.; Popić, J.; Garaj-Vrhovac, V. Apigenin: A Dietary Flavonoid with Diverse Anticancer Properties. *Cancer Lett.* 2018, *413*, 11–22.

28. Dobrzynska, M.; Napierala, M.; Florek, E. Flavonoid Nanoparticles: A Promising Approach for Cancer Therapy. *Biomolecules* **2020**, *10*, 1–17, doi:10.3390/biom10091268.

29. Imran, M.; Rauf, A.; Abu-Izneid, T.; Nadeem, M.; Shariati, M.A.; Khan, I.A.; Imran, A.; Orhan, I.E.; Rizwan, M.; Atif, M.; et al. Luteolin, a Flavonoid, as an Anticancer Agent: A Review. *Biomed. Pharmacother.* **2019**, *112*, doi:10.1016/j.biopha.2019.108612.

30. Veeramuthu, D.; Raja, W.R.T.; Al-Dhabi, N.A.; Savarimuthu, I. Flavonoids: Anticancer Properties. In *Flavonoids - From Biosynthesis to Human Health*; InTech, 2017.

31. Ramos, S. Effects of Dietary Flavonoids on Apoptotic Pathways Related to Cancer Chemoprevention. *J. Nutr. Biochem.* **2007**, *18*, 427–442, doi:10.1016/j.jnutbio.2006.11.004.

32. Cahyana, Y.; Adiyanti, T. Review: Flavonoids as Antidiabetic Agents. *Indones. J. Chem.* **2021**, *21*, 512–526, doi:10.22146/ijc.58439.

33. Gomes, D.; Silvestre, S.; Duarte, A.P.; Venuti, A.; Soares, C.P.; Passarinha, L.; Sousa, Â. In Silico Approaches: A Way to Unveil Novel Therapeutic Drugs for Cervical Cancer Management. *Pharmaceuticals* **2021**, *14*, doi:10.3390/ph14080741.

34. Najafi, M.; Tavakol, S.; Zarrabi, A.; Ashrafizadeh, M. Dual Role of Quercetin in Enhancing the Efficacy of Cisplatin in Chemotherapy and Protection against Its Side Effects: A Review. *Arch. Physiol. Biochem.* **2020**, *0*, 1–15, doi:10.1080/13813455.2020.1773864.

35. Siddiqui, M.; Abdellatif, B.; Zhai, K.; Liskova, A.; Kubatka, P.; Büsselberg, D. Flavonoids Alleviate Peripheral Neuropathy Induced by Anticancer Drugs. *Cancers (Basel).* **2021**, *13*, 1–36, doi:10.3390/cancers13071576.

36. Navarro-Hortal, M.D.; Varela-López, A.; Romero-Márquez, J.M.; Rivas-García, L.; Speranza, L.; Battino, M.; Quiles, J.L. Role of Flavonoids against Adriamycin Toxicity. *Food Chem. Toxicol.* **2020**, *146*, doi:10.1016/j.fct.2020.111820.

37. Cossarizza, A.; Gibellini, L.; Pinti, M.; Nasi, M.; Montagna, J.P.; De Biasi, S.; Roat, E.; Bertoncelli, L.; Cooper, E.L. Quercetin and Cancer Chemoprevention. *Evidence-based Complement. Altern. Med.* **2011**, *2011*, doi:10.1093/ECAM/NEQ053.

38. Seleem, D.; Pardi, V.; Murata, R.M. Review of Flavonoids: A Diverse Group of Natural

Compounds with Anti-Candida Albicans Activity in Vitro. *Arch. Oral Biol.* **2017**, *76*, 76–83, doi:10.1016/j.archoralbio.2016.08.030.

39. Liskova, A.; Samec, M.; Koklesova, L.; Brockmueller, A.; Zhai, K.; Abdellatif, B.; Siddiqui, M.; Biringer, K.; Kudela, E.; Pec, M.; et al. Flavonoids as an Effective Sensitizer for Anti-Cancer Therapy: Insights into Multi-Faceted Mechanisms and Applicability towards Individualized Patient Profiles. *EPMA J.* **2021**, *12*, 155–176, doi:10.1007/s13167-021-00242-5.

40. Panche, A.N.; Diwan, A.D.; Chandra, S.R. Flavonoids: An Overview. *J. Nutr. Sci.* 2016, *5*.

41. Clemente-Soto, A.F.; Salas-Vidal, E.; Milan-Pacheco, C.; Sánchez-Carranza, J.N.; Peralta-Zaragoza, O.; González-Maya, L. Quercetin Induces G2 Phase Arrest and Apoptosis with the Activation of P53 in an E6 Expression-Independent Manner in HPV-Positive Human Cervical Cancer-Derived Cells. *Mol. Med. Rep.* **2019**, *19*, 2097–2106, doi:10.3892/mmr.2019.9850.

42. Baksi, R.; Singh, D.P.; Borse, S.P.; Rana, R.; Sharma, V.; Nivsarkar, M. In Vitro and in Vivo Anticancer Efficacy Potential of Quercetin Loaded Polymeric Nanoparticles. *Biomed. Pharmacother.* **2018**, *106*, 1513–1526, doi:10.1016/j.biopha.2018.07.106.

43. Zhao, J.; Fang, Z.; Zha, Z.; Sun, Q.; Wang, H.; Sun, M.; Qiao, B. Quercetin Inhibits Cell Viability, Migration and Invasion by Regulating MiR-16/HOXA10 Axis in Oral Cancer. *Eur. J. Pharmacol.* **2019**, *847*, 11–18, doi:10.1016/j.ejphar.2019.01.006.

44. Hsiao, Y.C.; Kuo, W.H.; Chen, P.N.; Chang, H.R.; Lin, T.H.; Yang, W.E.; Hsieh, Y.S.; Chu, S.C. Flavanone and 2′-OH Flavanone Inhibit Metastasis of Lung Cancer Cells via down-Regulation of Proteinases Activities and MAPK Pathway. *Chem. Biol. Interact.* **2007**, *167*, 193–206, doi:10.1016/j.cbi.2007.02.012.

45. Cayetano-Salazar, L.; Olea-Flores, M.; Zuñiga-Eulogio, M.D.; Weinstein-Oppenheimer, C.; Fernández-Tilapa, G.; Mendoza-Catalán, M.A.; Zacapala-Gómez, A.E.; Ortiz-Ortiz, J.; Ortuño-Pineda, C.; Navarro-Tito, N. Natural Isoflavonoids in Invasive Cancer Therapy: From Bench to Bedside. *Phyther. Res.* 2021, *35*, 4092–4110.

46. Miadoková, E. Isoflavonoids - an Overview of Their Biological Activities and Potential Health Benefits. *Interdiscip. Toxicol.* **2009**, *2*, 211–218, doi:10.2478/v10102-009-0021-3.

47. Heiss, C.; Keen, C.L.; Kelm, M. Flavanols and Cardiovascular Disease Prevention. *Eur. Heart J.* 2010, *31*, 2583–2592.

48. Ferreira, M.K.A.; Fontenelle, R.O.S.; Magalhães, F.E.A.; Bandeira, P.N.; De Menezes, J.S.E.A.; Dos Santos, H.S. Chalcones Pharmacological Potential: A Brief Review. *Rev. Virtual Quim.* **2018**, *10*, 1455–1473, doi:10.21577/1984-6835.20180099.

49. Kuber Banoth, R.; Thatikonda, A. A REVIEW ON NATURAL CHALCONES AN UPDATE. *Int. J. Pharm. Sci. Res.* **2020**, *11*, 546, doi:10.13040/IJPSR.0975-8232.11(2).546-55.

50. Kopustinskiene, D.M.; Jakstas, V.; Savickas, A.; Bernatoniene, J. Flavonoids as Anticancer Agents. *Nutrients* 2020, *12*.

51. Sinopoli, A.; Calogero, G.; Bartolotta, A. Computational Aspects of Anthocyanidins and Anthocyanins: A Review. *Food Chem.* 2019, *297*.

52. dos Santos Lima, B.; Shanmugam, S.; de Souza Siqueira Quintans, J.; Quintans-Júnior, L.J.; de Souza Araújo, A.A. Inclusion Complex with Cyclodextrins Enhances the Bioavailability of Flavonoid Compounds: A Systematic Review. *Phytochem. Rev.* 2019, *18*, 1337–1359.

53. Thilakarathna, S.H.; Vasantha Rupasinghe, H.P. Flavonoid Bioavailability and Attempts for Bioavailability Enhancement. *Nutrients* 2013, *5*, 3367–3387.

54. Ding, Y.; Tong, Z.; Jin, L.; Ye, B.; Zhou, J.; Sun, Z.; Yang, H.; Hong, L.; Huang, F.; Wang, W.; et al. An NIR Discrete Metallacycle Constructed from Perylene Bisimide and Tetraphenylethylene Fluorophores for Imaging-Guided Cancer Radio-Chemotherapy. *Adv. Mater.* **2022**, *34*, 2106388, doi:10.1002/ADMA.202106388.

55. Zhou, J.; Yu, G.; Yang, J.; Shi, B.; Ye, B.; Wang, M.; Huang, F.; Stang, P.J. Polymeric Nanoparticles Integrated from Discrete Organoplatinum(II) Metallacycle by Stepwise Post-Assembly Polymerization for Synergistic Cancer Therapy. *Chem. Mater.* **2020**, *32*, 4564–4573, doi:10.1021/acs.chemmater.0c00615.

56. Zhou, J.; Rao, L.; Yu, G.; Cook, T.R.; Chen, X.; Huang, F. Supramolecular Cancer Nanotheranostics. *Chem. Soc. Rev.* **2021**, *50*, 2839–2891, doi:10.1039/d0cs00011f.

57. Khan, H.; Ullah, H.; Martorell, M.; Valdes, S.E.; Belwal, T.; Tejada, S.; Sureda, A.; Kamal, M.A. Flavonoids Nanoparticles in Cancer: Treatment, Prevention and Clinical Prospects. *Semin. Cancer Biol.* **2021**, *69*, 200–211, doi:10.1016/j.semcancer.2019.07.023.

58. Li, J.; Shi, M.; Ma, B.; Niu, R.; Zhang, H.; Kun, L. Antitumor Activity and Safety Evaluation of Nanaparticle-Based Delivery of Quercetin through Intravenous Administration in Mice. *Mater. Sci. Eng. C* **2017**, *77*, 803–810, doi:10.1016/j.msec.2017.03.191.

59. Li, J.; Li, Z.; Gao, Y.; Liu, S.; Li, K.; Wang, S.; Gao, L.; Shi, M.; Liu, Z.; Han, Z.; et al. Effect of a Drug Delivery System Made of Quercetin Formulated into PEGylation Liposomes on Cervical Carcinoma in Vitro and in Vivo. *J. Nanomater.* **2021**, *2021*, doi:10.1155/2021/9389934.

60. Saraswat, A.L.; Maher, T.J. Development and Optimization of Stealth Liposomal System for Enhanced in Vitro Cytotoxic Effect of Quercetin. *J. Drug Deliv. Sci. Technol.* **2020**, *55*, doi:10.1016/j.jddst.2019.101477.

61. Ding, B.; Chen, P.; Kong, Y.; Zhai, Y.; Pang, X.; Dou, J.; Zhai, G. Preparation and Evaluation of Folate-Modified Lipid Nanocapsules for Quercetin Delivery. *J. Drug Target.* **2014**, *22*, 67–75, doi:10.3109/1061186X.2013.839685.

62. Li, K.; Zhang, H.; Gao, L.; Zhai, Y.; Shi, M.; Li, J.; Xiu, C.; Cao, J.; Cheng, S.; Jiang, L.; et al. Preparation and Characterization of Baicalein-Loaded Nanoliposomes for Antitumor Therapy. *J. Nanomater.* **2016**, *2016*, doi:10.1155/2016/2861915.

63. Ni, S.; Hu, C.; Sun, R.; Zhao, G.; Xia, Q. Nanoemulsions-Based Delivery Systems for Encapsulation of Quercetin: Preparation, Characterization, and Cytotoxicity Studies. *J. Food Process Eng.* **2017**, *40*, doi:10.1111/jfpe.12374.

64. Rahimi, S.; Khoee, S.; Ghandi, M. Preparation and Characterization of Rod-like Chitosan–Quinoline Nanoparticles as PH-Responsive Nanocarriers for Quercetin Delivery. *Int. J. Biol. Macromol.* **2019**, *128*, 279–289, doi:10.1016/j.ijbiomac.2019.01.137.

65. Kunjiappan, S.; Panneerselvam, T.; Somasundaram, B.; Sankaranarayanan, M.; Chowdhury, R.; Chowdhury, A. *Design, Insilico Modeling, Biodistribution Study of Rutin and Quercetin Loaded-Stable Human Hair Keratin Nanoparticles Intended for Anticancer Drug Delivery*;

66. Deepika, M.S.; Thangam, R.; Sheena, T.S.; Sasirekha, R.; Sivasubramanian, S.; Babu, M.D.; Jeganathan, K.; Thirumurugan, R. A Novel Rutin-Fucoidan Complex Based Phytotherapy for Cervical Cancer through Achieving Enhanced Bioavailability and Cancer Cell Apoptosis. *Biomed. Pharmacother.* **2019**, *109*, 1181–1195, doi:10.1016/j.biopha.2018.10.178.

67. Fuster, M.G.; Carissimi, G.; Montalbán, M.G.; Víllora, G. Improving Anticancer Therapy with Naringenin-Loaded Silk Fibroin Nanoparticles. *Nanomaterials* **2020**, *10*, doi:10.3390/nano10040718.

68. Filho, I.K.; Machado, C.S.; Diedrich, C.; Karam, T.K.; Nakamura, C.V.; Khalil, N.M.; Mainardes, R.M. Optimized Chitosan-Coated Gliadin Nanoparticles Improved the Hesperidin Cytotoxicity over Tumor Cells. *Brazilian Arch. Biol. Technol.* **2021**, *64*, 1–14, doi:10.1590/1678-4324-75years-2021200795.

69. Zhang, H.; Liu, G.; Zeng, X.; Wu, Y.; Yang, C.; Mei, L.; Wang, Z.; Huang, L. Fabrication of Genistein-Loaded Biodegradable TPGS-b-PCL Nanoparticles for Improved Therapeutic Effects in Cervical Cancer Cells. *Int. J. Nanomedicine* **2015**, *10*, 2461–2473, doi:10.2147/IJN.S78988.

70. Van Thoai, D.; Nguyen, D.T.; Dang, L.H.; Nguyen, N.H.; Nguyen, V.T.; Doan, P.; Nguyen, B.T.; Le Van Thu; Tung, N.N.; Quyen, T.N. Lipophilic Effect of Various Pluronic-Grafted Gelatin Copolymers on the Quercetin Delivery Efficiency in These Self-Assembly Nanogels. *J. Polym. Res.* **2020**, *27*, doi:10.1007/s10965-020-02216-z.

71. El-Gogary, R.I.; Rubio, N.; Wang, J.T.W.; Al-Jamal, W.T.; Bourgognon, M.; Kafa, H.; Naeem, M.; Klippstein, R.; Abbate, V.; Leroux, F.; et al. Polyethylene Glycol Conjugated Polymeric Nanocapsules for Targeted Delivery of Quercetin to Folate-Expressing Cancer Cells in Vitro and in Vivo. *ACS Nano* **2014**, *8*, 1384–1401, doi:10.1021/nn405155b.

72. Ghafelehbashi, R.; Tavakkoli Yaraki, M.; Heidarpoor Saremi, L.; Lajevardi, A.; Haratian, M.; Astinchap, B.; Rashidi, A.M.; Moradian, R. A PH-Responsive Citric-Acid/α-Cyclodextrin-Functionalized Fe3O4 Nanoparticles as a Nanocarrier for Quercetin: An Experimental and DFT Study. *Mater. Sci. Eng. C* **2020**, *109*, doi:10.1016/j.msec.2019.110597.

73. Payne, J.N.; Badwaik, V.D.; Waghwani, H.K.; Moolani, H. V.; Tockstein, S.; Thompson, D.H.; Dakshinamurthy, R. Development of Dihydrochalcone-Functionalized Gold Nanoparticles for Augmented Antineoplastic Activity. *Int. J. Nanomedicine* **2018**, *13*, 1917–1926, doi:10.2147/IJN.S143506.

74. Wang, H.; Tan, M.; Zhu, J.; Pan, Y.; Chen, Z.; Liang, H.; Liu, H. Synthesis, Cytotoxic Activity, and DNA Binding Properties of Copper (II) Complexes with Hesperetin, Naringenin, and Apigenin. *Bioinorg. Chem. Appl.* **2009**, *2009*, doi:10.1155/2009/347872.

75. Simon, A.T.; Dutta, D.; Chattopadhyay, A.; Ghosh, S.S. Quercetin-Loaded Luminescent Hydroxyapatite Nanoparticles for Theranostic Application in Monolayer and Spheroid Cultures of Cervical Cancer Cell Line in Vitro. *ACS Appl. Bio Mater.* **2021**, *4*, 4495–4506, doi:10.1021/acsabm.1c00255.

76. Mashhadi Malekzadeh, A.; Ramazani, A.; Tabatabaei Rezaei, S.J.; Niknejad, H. Design and Construction of Multifunctional Hyperbranched Polymers Coated Magnetite Nanoparticles for Both Targeting Magnetic Resonance Imaging and Cancer Therapy. *J. Colloid Interface Sci.* **2017**, *490*, 64–73, doi:10.1016/j.jcis.2016.11.014.

77. Yamina, A.M.; Fizir, M.; Itatahine, A.; He, H.; Dramou, P. Preparation of Multifunctional PEG-Graft-Halloysite Nanotubes for Controlled Drug Release, Tumor Cell Targeting, and Bio-Imaging. *Colloids Surfaces B Biointerfaces* **2018**, *170*, 322–329, doi:10.1016/j.colsurfb.2018.06.042.

78. Akal, Z.; Alpsoy, L.; Baykal, A. Biomedical Applications of SPION@APTES@PEG-Folic Acid@carboxylated Quercetin Nanodrug on Various Cancer Cells. *Appl. Surf. Sci.* **2016**, *378*, 572–581, doi:10.1016/j.apsusc.2016.03.217.

79. Alpsoy, L.; Baykal, A.; Kurtan, U.; Ülker, Z. Synthesis and Characterization of Carboxylated Luteolin (CL)-Functionalized SPION. *J. Supercond. Nov. Magn.* **2017**, *30*, 2797–2804, doi:10.1007/s10948-017-4056-y.

80. Yu, C.; Gao, C.; Lü, S.; Chen, C.; Huang, Y.; Liu, M. Redox-Responsive Shell-Sheddable Micelles Self-Assembled from Amphiphilic Chondroitin Sulfate-Cholesterol Conjugates for Triggered Intracellular Drug Release. *Chem. Eng. J.* **2013**, *228*, 290–299, doi:10.1016/j.cej.2013.04.083.

81. Jeong, D.; Choi, J.M.; Choi, Y.; Jeong, K.; Cho, E.; Jung, S. Complexation of Fisetin with Novel Cyclosophoroase Dimer to Improve Solubility and Bioavailability. *Carbohydr. Polym.* **2013**, *97*, 196–202, doi:10.1016/j.carbpol.2013.04.066.

82. Sundararajan, M.; Thomas, P.A.; Venkadeswaran, K.; Jeganathan, K.; Geraldine, P. Synthesis and Characterization of Chrysin-Loaded β-Cyclodextrin-Based Nanosponges to Enhance in-Vitro Solubility, Photostability, Drug Release, Antioxidant Effects and Antitumorous Efficacy. *J. Nanosci. Nanotechnol.* **2017**, *17*, 8742–8751, doi:10.1166/jnn.2017.13911.

83. Lv, T.; Yu, T.; Fang, Y.; Zhang, S.; Jiang, M.; Zhang, H.; Zhang, Y.; Li, Z.; Chen, H.; Gao, Y. Role of Generation on Folic Acid-Modified Poly(Amidoamine) Dendrimers for Targeted Delivery of Baicalin to Cancer Cells. *Mater. Sci. Eng. C* **2017**, *75*, 182–190, doi:10.1016/j.msec.2016.12.134.

84. Wang, W.; Sun, C.; Mao, L.; Ma, P.; Liu, F.; Yang, J.; Gao, Y. The Biological Activities, Chemical Stability, Metabolism and Delivery Systems of Quercetin: A Review. *Trends Food Sci. Technol.* **2016**, *56*, 21–38, doi:10.1016/j.tifs.2016.07.004.

85. Caballero, S.; Li, Y.O.; McClements, D.J.; Davidov-Pardo, G. Encapsulation and Delivery of Bioactive Citrus Pomace Polyphenols: A Review. *Crit. Rev. Food Sci. Nutr.* **2021**, *0*, 1–17, doi:10.1080/10408398.2021.1922873.

86. Katopodi, A.; Detsi, A. Solid Lipid Nanoparticles and Nanostructured Lipid Carriers of Natural Products as Promising Systems for Their Bioactivity Enhancement: The Case of Essential Oils and Flavonoids. *Colloids Surfaces A Physicochem. Eng. Asp.* **2021**, *630*, 127529, doi:10.1016/j.colsurfa.2021.127529.

87. Patel, G.; Thakur, N.S.; Kushwah, V.; Patil, M.D.; Nile, S.H.; Jain, S.; Banerjee, U.C.; Kai, G. Liposomal Delivery of Mycophenolic Acid With Quercetin for Improved Breast Cancer Therapy in SD Rats. *Front. Bioeng. Biotechnol.* **2020**, *8*, 1–15, doi:10.3389/fbioe.2020.00631.

88. Hu, J.; Wang, J.; Wang, G.; Yao, Z.; Dang, X. Pharmacokinetics and Antitumor Efficacy of DSPE-PEG2000 Polymeric Liposomes Loaded with Quercetin and Temozolomide: Analysis of Their Effectiveness in Enhancing the Chemosensitization of Drug-Resistant Glioma Cells. *Int. J. Mol. Med.* **2016**, *37*, 690–702, doi:10.3892/ijmm.2016.2458.

89. Rezaei-Sadabady, R.; Eidi, A.; Zarghami, N.; Barzegar, A. Intracellular ROS Protection Efficiency and Free Radical-Scavenging Activity of Quercetin and Quercetin-Encapsulated Liposomes. *Artif. Cells, Nanomedicine Biotechnol.* **2016**, *44*, 128–134, doi:10.3109/21691401.2014.926456.

90. Bazylińska, U.; Pucek, A.; Sowa, M.; Matczak-Jon, E.; Wilk, K.A. Engineering of Phosphatidylcholine-Based Solid Lipid Nanocarriers for Flavonoids Delivery. *Colloids Surfaces A Physicochem. Eng. Asp.* **2014**, *460*, 483–493, doi:10.1016/j.colsurfa.2014.02.034.

91. Fathi, M.; Varshosaz, J.; Mohebbi, M.; Shahidi, F. Hesperetin-Loaded Solid Lipid Nanoparticles and Nanostructure Lipid Carriers for Food Fortification: Preparation, Characterization, and Modeling. *Food Bioprocess Technol.* **2013**, *6*, 1464–1475,

doi:10.1007/s11947-012-0845-2.

92. Bose, S.; Du, Y.; Takhistov, P.; Michniak-Kohn, B. Formulation Optimization and Topical Delivery of Quercetin from Solid Lipid Based Nanosystems. *Int. J. Pharm.* **2013**, *441*, 56–66, doi:10.1016/j.ijpharm.2012.12.013.

93. Scalia, S.; Haghi, M.; Losi, V.; Trotta, V.; Young, P.M.; Traini, D. Quercetin Solid Lipid Microparticles: A Flavonoid for Inhalation Lung Delivery. *Eur. J. Pharm. Sci.* **2013**, *49*, 278–285, doi:10.1016/j.ejps.2013.03.009.

94. Sun, M.; Nie, S.; Pan, X.; Zhang, R.; Fan, Z.; Wang, S. Quercetin-Nanostructured Lipid Carriers: Characteristics and Anti-Breast Cancer Activities in Vitro. *Colloids Surfaces B Biointerfaces* **2014**, *113*, 15–24, doi:10.1016/j.colsurfb.2013.08.032.

95. Liu, Y.; Zhang, H.; Cui, H.; Zhang, F.; Zhao, L.; Liu, Y.; Meng, Q. Combined and Targeted Drugs Delivery System for Colorectal Cancer Treatment: Conatumumab Decorated, Reactive Oxygen Species Sensitive Irinotecan Prodrug and Quercetin Co-Loaded Nanostructured Lipid Carriers. *Drug Deliv.* **2022**, *29*, 342–350, doi:10.1080/10717544.2022.2027573.

96. Firoozeh, N.; Mahmoud, O.; Layasadat, K.; Mohammadreza, A.; Esrafil, M.; Ali, K. E Ff Ects of Quercetin-Loaded Nanoparticles on MCF-7. *Medicina (B. Aires).* **2019**, *55*, 1–15.

97. Yostawonkul, J.; Surassmo, S.; Iempridee, T.; Pimtong, W.; Suktham, K.; Sajomsang, W.; Gonil, P.; Ruktanonchai, U.R. Surface Modification of Nanostructure Lipid Carrier (NLC) by Oleoyl-Quaternized-Chitosan as a Mucoadhesive Nanocarrier. *Colloids Surfaces B Biointerfaces* **2017**, *149*, 301–311, doi:10.1016/j.colsurfb.2016.09.049.

98. Dora, C.L.; Silva, L.F.C.; Mazzarino, L.; Siqueira, J.M.; Fernandes, D.; Pacheco, L.K.; Maioral, M.F.; Santos-Silva, M.C.; Baisch, A.L.M.; Assreuy, J.; et al. Oral Delivery of a High Quercetin Payload Nanosized Emulsion: In Vitro and in Vivo Activity against B16-F10 Melanoma. *J. Nanosci. Nanotechnol.* **2016**, *16*, 1275–1281, doi:10.1166/jnn.2016.11675.

99. Qian, C.; McClements, D.J. Formation of Nanoemulsions Stabilized by Model Food-Grade Emulsifiers Using High-Pressure Homogenization: Factors Affecting Particle Size. *Food Hydrocoll.* **2011**, *25*, 1000–1008, doi:10.1016/j.foodhyd.2010.09.017.

100. Ting, Y.; Chiou, Y.S.; Pan, M.H.; Ho, C.T.; Huang, Q. In Vitro and in Vivo Anti-Cancer Activity of Tangeretin against Colorectal Cancer Was Enhanced by Emulsion-Based Delivery System. *J. Funct. Foods* **2015**, *15*, 264–273, doi:10.1016/j.jff.2015.03.034.

101. Ragelle, H.; Crauste-Manciet, S.; Seguin, J.; Brossard, D.; Scherman, D.; Arnaud, P.; Chabot, G.G. Nanoemulsion Formulation of Fisetin Improves Bioavailability and Antitumour Activity in Mice. *Int. J. Pharm.* **2012**, *427*, 452–459, doi:10.1016/j.ijpharm.2012.02.025.

102. Wang, Q.; Bao, Y.; Ahire, J.; Chao, Y. Co-Encapsulation of Biodegradable Nanoparticles with Silicon Quantum Dots and Quercetin for Monitored Delivery. *Adv. Healthc. Mater.*

2013, *2*, 459–466, doi:10.1002/adhm.201200178.

103. Kim, E.S.; Kim, D.Y.; Lee, J.S.; Lee, H.G. Quercetin Delivery Characteristics of Chitosan Nanoparticles Prepared with Different Molecular Weight Polyanion Cross-Linkers. *Carbohydr. Polym.* **2021**, *267*, doi:10.1016/j.carbpol.2021.118157.

104. Singh, A.; Dutta, P.K.; Kumar, H.; Kureel, A.K.; Rai, A.K. Synthesis of Chitin-Glucan-Aldehyde-Quercetin Conjugate and Evaluation of Anticancer and Antioxidant Activities. *Carbohydr. Polym.* **2018**, *193*, 99–107, doi:10.1016/j.carbpol.2018.03.092.

105. de Oliveira Pedro, R.; Hoffmann, S.; Pereira, S.; Goycoolea, F.M.; Schmitt, C.C.; Neumann, M.G. Self-Assembled Amphiphilic Chitosan Nanoparticles for Quercetin Delivery to Breast Cancer Cells. *Eur. J. Pharm. Biopharm.* **2018**, *131*, 203–210, doi:10.1016/j.ejpb.2018.08.009.

106. Nguyen, H.T.; Goycoolea, F.M. Chitosan/Cyclodextrin/TPP Nanoparticles Loaded with Quercetin as Novel Bacterial Quorum Sensing Inhibitors. *Molecules* **2017**, *22*, 1–23, doi:10.3390/molecules22111975.

107. Krauland, A.H.; Alonso, M.J. Chitosan/Cyclodextrin Nanoparticles as Macromolecular Drug Delivery System. *Int. J. Pharm.* **2007**, *340*, 134–142, doi:10.1016/j.ijpharm.2007.03.005.

108. Fülöp, Z.; Saokham, P.; Loftsson, T. Sulfobutylether-β-Cyclodextrin/Chitosan Nano- and Microparticles and Their Physicochemical Characteristics. *Int. J. Pharm.* **2014**, *472*, 282–287, doi:10.1016/j.ijpharm.2014.06.039.

109. Zhang, X.; Xu, M.; Zhang, Z.; Hu, X.; Hao, L.; Lin, Q.; Wang, S.; Jiang, W. Preparation and Characterization of Magnetic Fluorescent Microspheres for Delivery of Kaempferol. *Mater. Technol.* **2017**, *32*, 125–130, doi:10.1080/10667857.2016.1157913.

110. Qureshi, W.A.; Zhao, R.; Wang, H.; Ji, T.; Ding, Y.; Ihsan, A.; Mujeeb, A.; Nie, G.; Zhao, Y. Co-Delivery of Doxorubicin and Quercetin via MPEG–PLGA Copolymer Assembly for Synergistic Anti-Tumor Efficacy and Reducing Cardio-Toxicity. *Sci. Bull.* **2016**, *61*, 1689–1698, doi:10.1007/s11434-016-1182-z.

111. Liu, Y.; Liu, C.; Tang, C.; Yin, C. Dual Stimulus-Responsive Chitosan-Based Nanoparticles Co-Delivering Doxorubicin and Quercetin for Cancer Therapy. *Mater. Lett.* **2021**, *305*, 130826, doi:10.1016/j.matlet.2021.130826.

112. Konecsni, K.; Low, N.H.; Nickerson, M.T. Chitosan-Tripolyphosphate Submicron Particles as the Carrier of Entrapped Rutin. *Food Chem.* **2012**, *134*, 1775–1779, doi:10.1016/j.foodchem.2012.03.070.

113. Bi, F.; Yong, H.; Liu, J.; Zhang, X.; Shu, Y.; Liu, J. Development and Characterization of Chitosan and D-α-Tocopheryl Polyethylene Glycol 1000 Succinate Composite Films Containing Different Flavones. *Food Packag. Shelf Life* **2020**, *25*, doi:10.1016/j.fpsl.2020.100531.

114. Saha, C.; Kaushik, A.; Das, A.; Pal, S.; Majumder, D. Anthracycline Drugs on Modified Surface of Quercetin-Loaded Polymer Nanoparticles: A Dual Drug Delivery Model for Cancer Treatment. *PLoS One* **2016**, *11*, 1–15, doi:10.1371/journal.pone.0155710.

115. Karthick, V.; Panda, S.; Kumar, V.G.; Kumar, D.; Shrestha, L.K.; Ariga, K.; Vasanth, K.; Chinnathambi, S.; Dhas, T.S.; Suganya, K.S.U. Quercetin Loaded PLGA Microspheres Induce Apoptosis in Breast Cancer Cells. *Appl. Surf. Sci.* **2019**, *487*, 211–217, doi:10.1016/j.apsusc.2019.05.047.

116. Sunoqrot, S.; Abujamous, L. PH-Sensitive Polymeric Nanoparticles of Quercetin as a Potential Colon Cancer-Targeted Nanomedicine. *J. Drug Deliv. Sci. Technol.* **2019**, *52*, 670–676, doi:10.1016/j.jddst.2019.05.035.

117. Pandey, S.K.; Patel, D.K.; Thakur, R.; Mishra, D.P.; Maiti, P.; Haldar, C. Anti-Cancer Evaluation of Quercetin Embedded PLA Nanoparticles Synthesized by Emulsified Nanoprecipitation. *Int. J. Biol. Macromol.* **2015**, *75*, 521–529, doi:10.1016/j.ijbiomac.2015.02.011.

118. Chen, L.C.; Chen, Y.C.; Su, C.Y.; Hong, C.S.; Ho, H.O.; Sheu, M.T. Development and Characterization of Self-Assembling Lecithin-Based Mixed Polymeric Micelles Containing Quercetin in Cancer Treatment and an in Vivo Pharmacokinetic Study. *Int. J. Nanomedicine* **2016**, *11*, 1557–1566, doi:10.2147/IJN.S103681.

119. Patra, A.; Satpathy, S.; Shenoy, A.K.; Bush, J.A.; Kazi, M.; Hussain, M.D. Formulation and Evaluation of Mixed Polymeric Micelles of Quercetin for Treatment of Breast, Ovarian, and Multidrug Resistant Cancers. *Int. J. Nanomedicine* **2018**, *13*, 2869–2881, doi:10.2147/IJN.S153094.

120. Cote, B.; Carlson, L.J.; Rao, D.A.; Alani, A.W.G. Combinatorial Resveratrol and Quercetin Polymeric Micelles Mitigate Doxorubicin Induced Cardiotoxicity in Vitro and in Vivo. *J. Control. Release* **2015**, *213*, 128–133, doi:10.1016/j.jconrel.2015.06.040.

121. Zhao, M.H.; Yuan, L.; Meng, L.Y.; Qiu, J.L.; Wang, C. Bin Quercetin-Loaded Mixed Micelles Exhibit Enhanced Cytotoxic Efficacy in Non-Small Cell Lung Cancer in Vitro. *Exp. Ther. Med.* **2017**, *14*, 5503–5508, doi:10.3892/etm.2017.5230.

122. Khonkarn, R.; Mankhetkorn, S.; Hennink, W.E.; Okonogi, S. PEG-OCL Micelles for Quercetin Solubilization and Inhibition of Cancer Cell Growth. *Eur. J. Pharm. Biopharm.* **2011**, *79*, 268–275, doi:10.1016/j.ejpb.2011.04.011.

123. Xu, G.Y.; Shi, H.S.; Ren, L. Bin; Gou, H.F.; Gong, D.Y.; Gao, X.; Huang, N. Enhancing the Anti-Colon Cancer Activity of Quercetin by Self-Assembled Micelles. *Int. J. Nanomedicine* **2015**, *10*, 2051–2063, doi:10.2147/IJN.S75550.

124. Trapani, A.; Lopedota, A.; Franco, M.; Cioffi, N.; Ieva, E.; Garcia-Fuentes, M.; Alonso, M.J. A Comparative Study of Chitosan and Chitosan/Cyclodextrin Nanoparticles as Potential Carriers for the Oral Delivery of Small Peptides. *Eur. J. Pharm. Biopharm.* **2010**, *75*, 26–32, doi:10.1016/j.ejpb.2010.01.010.

125. Trapani, A.; Garcia-Fuentes, M.; Alonso, M.J. Novel Drug Nanocarriers Combining Hydrophilic Cyclodextrins and Chitosan. *Nanotechnology* **2008**, *19*, doi:10.1088/0957-4484/19/18/185101.

126. Zhu, P.; Chen, L.; Zhao, Y.; Gao, C.; Yang, J.; Liao, X.; Liu, D.; Yang, B. A Novel Host-Guest Complex Based on Biotin Functionalized Polyamine-β-Cyclodextrin for Tumor Targeted Delivery of Luteolin. *J. Mol. Struct.* **2021**, *1237*, 130339, doi:10.1016/j.molstruc.2021.130339.

127. Liu, B.; Li, W.; Zhao, J.; Liu, Y.; Zhu, X.; Liang, G. Physicochemical Characterisation of the Supramolecular Structure of Luteolin/Cyclodextrin Inclusion Complex. *Food Chem.* **2013**, *141*, 940–945, doi:10.1016/j.foodchem.2013.03.097.

128. D'Onofre Couto, B.; Novaes da Costa, R.; Castro Laurindo, W.; Moraes da Silva, H.; Rocha da Silva, C.; Sélia dos Reis Coimbra, J.; Barbosa Mageste, A.; de Cássia Dias, S.; José Boggione Santos, I. Characterization, Techno-Functional Properties, and Encapsulation Efficiency of Self-Assembled β-Lactoglobulin Nanostructures. *Food Chem.* **2021**, *356*, doi:10.1016/j.foodchem.2021.129719.

129. Zu, Y.; Wu, W.; Zhao, X.; Li, Y.; Zhong, C.; Zhang, Y. The High Water Solubility of Inclusion Complex of Taxifolin-γ-CD Prepared and Characterized by the Emulsion Solvent Evaporation and the Freeze Drying Combination Method. *Int. J. Pharm.* **2014**, *477*, 148–158, doi:10.1016/j.ijpharm.2014.10.027.

130. Chem, A.J.; Liu, M.; Liao, A.R.; Zhao, A.Y.; A, B.Y. Host – Guest Inclusion System of Luteolin with Polyamine- b -Cyclodextrin : Preparation , Characterisation , Anti-Oxidant and Anti-Cancer Activity. **2015**.

131. Luong, D.; Kesharwani, P.; Deshmukh, R.; Mohd Amin, M.C.I.; Gupta, U.; Greish, K.; Iyer, A.K. PEGylated PAMAM Dendrimers: Enhancing Efficacy and Mitigating Toxicity for Effective Anticancer Drug and Gene Delivery. *Acta Biomater.* **2016**, *43*, 14–29, doi:10.1016/j.actbio.2016.07.015.

132. Chauhan, A.S. Dendrimers for Drug Delivery. *Molecules* **2018**, *23*, doi:10.3390/molecules23040938.

133. Grabovac, V.; Guggi, D.; Bernkop-Schnürch, A. Comparison of the Mucoadhesive Properties of Various Polymers. *Adv. Drug Deliv. Rev.* **2005**, *57*, 1713–1723, doi:10.1016/j.addr.2005.07.006.

134. Bonferoni, M.C.; Sandri, G.; Rossi, S.; Ferrari, F.; Caramella, C. Chitosan and Its Salts for Mucosal and Transmucosal Delivery. *Expert Opin. Drug Deliv.* **2009**, *6*, 923–939, doi:10.1517/17425240903114142.

135. Pedro, A.S.; Cabral-Albuquerque, E.; Ferreira, D.; Sarmento, B. Chitosan: An Option for Development of Essential Oil Delivery Systems for Oral Cavity Care? *Carbohydr. Polym.* **2009**, *76*, 501–508, doi:10.1016/j.carbpol.2008.12.016.

136. Rodolfo, C.; Eusébio, D.; Ventura, C.; Nunes, R.; Florindo, H.F.; Costa, D.; Sousa, Â.

Design of Experiments to Achieve an Efficient Chitosan-Based Dna Vaccine Delivery System. *Pharmaceutics* **2021**, *13*, doi:10.3390/pharmaceutics13091369.

137. Nunes, R.; Serra, A.S.; Simaite, A.; Sousa, Â. Modulation of Chitosan-TPP Nanoparticle Properties for Plasmid DNA Vaccines Delivery. *Polymers (Basel).* **2022**, *14*, doi:10.3390/polym14071443.

138. Tomaz, A.F.; de Carvalho, S.M.S.; Barbosa, R.C.; Silva, S.M.L.; Gutierrez, M.A.S.; de Lima, A.G.B.; Fook, M.V.L. Ionically Crosslinked Chitosan Membranes Used as Drug Carriers for Cancer Therapy Application. *Materials (Basel).* **2018**, *11*, 1–18, doi:10.3390/ma11102051.

139. Zhao, D.; Yu, S.; Sun, B.; Gao, S.; Guo, S.; Zhao, K. Biomedical Applications of Chitosan and Its Derivative Nanoparticles. *Polymers (Basel).* **2018**, *10*, doi:10.3390/polym10040462.

140. Feng, H.; Zhang, L.; Zhu, C. Genipin Crosslinked Ethyl Cellulose-Chitosan Complex Microspheres for Anti-Tuberculosis Delivery. *Colloids Surfaces B Biointerfaces* **2013**, *103*, 530–537, doi:10.1016/j.colsurfb.2012.11.007.

141. Souza, M.P.; Vaz, A.F.M.; Correia, M.T.S.; Cerqueira, M.A.; Vicente, A.A.; Carneiro-da-Cunha, M.G. Quercetin-Loaded Lecithin/Chitosan Nanoparticles for Functional Food Applications. *Food Bioprocess Technol.* **2014**, *7*, 1149–1159, doi:10.1007/s11947-013-1160-2.

142. Marcucci, F.; Lefoulon, F. Active Targeting with Particulate Drug Carriers in Tumor Therapy: Fundamentals and Recent Progress. *Drug Discov. Today* **2004**, *9*, 219–228, doi:10.1016/S1359-6446(03)02988-X.

143. Prabha, S.; Arya, G.; Chandra, R.; Ahmed, B.; Nimesh, S. Effect of Size on Biological Properties of Nanoparticles Employed in Gene Delivery. *Artif. Cells, Nanomedicine Biotechnol.* **2016**, *44*, 83–91, doi:10.3109/21691401.2014.913054.

144. Zhao, F.; Zhao, Y.; Liu, Y.; Chang, X.; Chen, C.; Zhao, Y. Cellular Uptake, Intracellular Trafficking, and Cytotoxicity of Nanomaterials. *Small* **2011**, *7*, 1322–1337, doi:10.1002/smll.201100001.

145. Harush-Frenkel, O.; Debotton, N.; Benita, S.; Altschuler, Y. Targeting of Nanoparticles to the Clathrin-Mediated Endocytic Pathway. *Biochem. Biophys. Res. Commun.* **2007**, *353*, 26–32, doi:10.1016/j.bbrc.2006.11.135.

146. Clogston, J.D.; Patri, A.K. Zeta Potential Measurement. *Methods Mol. Biol.* **2011**, *697*, 63–70, doi:10.1007/978-1-60327-198-1_6.

147. Calvo, P.; Remun˜a´n, C.; Remun˜a, R.; Remun˜a´n-Lo´pez, R.; Lo´pez, L.; Vila-Jato, J.L.; Alonso, M.J. *Novel Hydrophilic Chitosan-Polyethylene Oxide Nanoparticles as Protein Carriers*;

148. Patel, A.R.; Heussen, P.C.M.; Hazekamp, J.; Drost, E.; Velikov, K.P. Quercetin Loaded

Biopolymeric Colloidal Particles Prepared by Simultaneous Precipitation of Quercetin with Hydrophobic Protein in Aqueous Medium. *Food Chem.* **2012**, *133*, 423–429, doi:10.1016/j.foodchem.2012.01.054.

149. Ibrahim, Y.H.E.Y.; Regdon, G.; Kristó, K.; Kelemen, A.; Adam, M.E.; Hamedelniel, E.I.; Sovány, T. Design and Characterization of Chitosan/Citrate Films as Carrier for Oral Macromolecule Delivery. *Eur. J. Pharm. Sci.* **2020**, *146*, 105270, doi:10.1016/j.ejps.2020.105270.

150. Loutfy, S.A.; Salaheldin, T.A.; Ramadan, M.A.; Farroh, K.Y.; Abdallah, Z.F.; Eloahed, T.Y.A. Synthesis, Characterization and Cytotoxic Evaluation of Graphene Oxide Nanosheets: In Vitro Liver Cancer Model. *Asian Pacific J. Cancer Prev.* **2017**, *18*, 955–961, doi:10.22034/APJCP.2017.18.4.955.

151. Ahmed, M.E.S.; Mohamed, H.M.; Mohamed, M.I.; Kandile, N.G. Sustainable Antimicrobial Modified Chitosan and Its Nanoparticles Hydrogels: Synthesis and Characterization. *Int. J. Biol. Macromol.* **2020**, *162*, 1388–1397, doi:10.1016/j.ijbiomac.2020.08.048.

152. Yang, Z.; Peng, H.; Wang, W.; Liu, T. Crystallization Behavior of Poly(ε-Caprolactone)/Layered Double Hydroxide Nanocomposites. *J. Appl. Polym. Sci.* **2010**, *116*, 2658–2667, doi:10.1002/app.

Chapter 7 - Annexes

Open Access Review

Flavonoids-Based Delivery Systems towards Cancer Therapies

by Miguel Ferreira, Diana Costa * and Ângela Sousa *

CICS-UBI—Health Science Research Centre, University of Beira Interior, Av. Infante D. Henrique, 6200-506 Covilhã, Portugal

* Authors to whom correspondence should be addressed.

Academic Editors: Wujie Zhang and Murugan Ramalingam

Bioengineering **2022**, *9*(5), 197; https://doi.org/10.3390/bioengineering9050197

Received: 29 March 2022 / Revised: 26 April 2022 / Accepted: 28 April 2022 / Published: 2 May 2022

(This article belongs to the Special Issue Drug Delivery Systems for Cancer Treatment)

View Full-Text | Download PDF | Browse Figures | Citation Export

Abstract

Cancer is the second leading cause of death worldwide. Cervical cancer, for instance, is considered a major scourge in low-income countries. Its development is mostly associated with the human papillomavirus persistent infection and despite the availability of preventive vaccines, they are only widely administered in more developed countries, thus leaving a large percentage of unvaccinated women highly susceptible to this type of cancer. Current treatments are based on invasive techniques, being far from effective. Therefore, the search for novel, advanced and personalized therapeutic approaches is imperative. Flavonoids belong to a group of natural polyphenolic compounds, well recognized for their great anticancer capacity, thus promising to be incorporated in cancer therapy protocols. However, their use is limited due to their low solubility, stability and bioavailability. To surpass these limitations, the encapsulation of flavonoids into delivery systems emerged as a valuable strategy to improve their stability and bioavailability. In this context, the aim of this review is to present the most reliable flavonoids-based delivery systems developed for anticancer therapies and the progress accomplished, with a special focus on cervical cancer therapy. The gathered information revealed the high therapeutic potential of flavonoids and highlights the relevance of delivery systems application, allowing a better understanding for future studies on effective cancer therapy. View Full-Text

Keywords: anticancer activity; cervical cancer; delivery systems; flavonoids; HeLa cells; tumor inhibition

▼ Show Figures

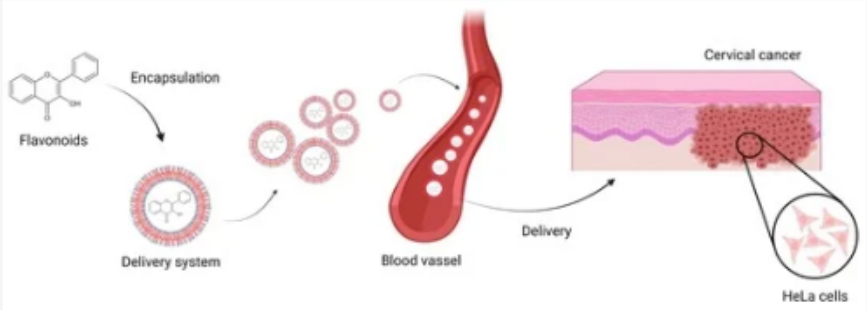

Graphical abstract